Detection of the HIV-1 accessory proteins Nef and Vpu by flow cytometry represents a new tool to study their functional interplay within a single infected CD4+ T cell

Jérémie Prévost[1,2,*], Jonathan Richard[1,2,*], Romain Gasser[1,2], Halima Medjahed[1], Frank Kirchhoff[3], Beatrice H. Hahn[4], John C. Kappes[5], Christina Ochsenbauer[5], Ralf Duerr[6], Andrés Finzi[1,2,7,#]

[1]Centre de Recherche du CHUM, Montreal, Quebec, Canada
[2]Département de Microbiologie, Infectiologie et Immunologie, Université de Montréal, Montreal, Quebec, Canada
[3]Institute of Molecular Virology, Ulm University Medical Center, Ulm, Germany.
[4]Departments of Medicine and Microbiology, Perelman School of Medicine, University of Pennsylvania, Philadelphia, PA, USA
[5]Department of Medicine, University of Alabama at Birmingham, Birmingham, AL, USA
[6]Department of Microbiology, New York University School of Medicine, New York, NY, USA
[7]Department of Microbiology and Immunology, McGill University, Montreal, Quebec, Canada

*Contributed equally

[#]**Corresponding author:**
Andrés Finzi
Centre de recherche du CHUM (CRCHUM)
900 St-Denis street, Tour Viger, R09.420
Montréal, Québec, H2X 0A9, Canada
andres.finzi@umontreal.ca
Phone: 514-890-8000 ext: 35264
Fax: 514-412-7936

Running Title: Nef and Vpu expression dictates ADCC responses

Key Words: HIV-1, Env, Nef, Vpu, CD4, BST-2, ADCC, LucR.T2A, non-neutralizing antibodies, CD4-bound conformation

ABSTRACT

The HIV-1 Nef and Vpu accessory proteins are known to protect infected cells from antibody-dependent cellular cytotoxicity (ADCC) responses by limiting exposure of CD4-induced (CD4i) envelope (Env) epitopes at the cell surface. Although both proteins target the host receptor CD4 for degradation, the extent of their functional redundancy is unknown. Here, we developed an intracellular staining technique that permits the intracellular detection of both Nef and Vpu in primary CD4+ T cells by flow cytometry. Using this method, we show that the combined expression of Nef and Vpu predicts the susceptibility of HIV-1-infected primary CD4+ T cells to ADCC by HIV+ plasma. We also show that Vpu cannot compensate for the absence of Nef, thus providing an explanation for why some infectious molecular clones that carry a LucR reporter gene upstream of Nef render infected cells more susceptible to ADCC responses. Our method thus represents a new tool to dissect the biological activity of Nef and Vpu in the context of other host and viral proteins within single infected CD4+ T cells.

IMPORTANCE

HIV-1 Nef and Vpu exert several biological functions that are important for viral immune evasion, release and replication. Here, we developed a new method allowing simultaneous detection of these accessory proteins in their native form together with some of their cellular substrates. This allowed us to show that Vpu cannot compensate the lack of a functional Nef, which has implication for studies that use Nef-defective viruses to study ADCC responses.

57 **INTRODUCTION**

58 The human immunodeficiency virus type 1 (HIV-1) genome encodes four accessory proteins
59 (Vif, Vpr, Vpu and Nef), which are dispensable for viral replication *in vitro* but required
60 for efficient replication, restriction factors counteraction and immune evasion *in vivo* (1-
61 7). Among them, Nef and Vpu are well known for their role in subverting the host cell
62 protein trafficking machinery (8, 9).

63

64 HIV-1 Nef is a small cytoplasmic protein of 27 kDa produced from early viral transcripts (10),
65 which requires a myristoyl group on its N-terminus to traffic to intracellular and plasma
66 membranes (11). Nef harbors a highly conserved dileucine motif in its C-terminal flexible loop
67 that is responsible for the interaction with clathrin adaptors protein complexes (AP-1, AP-2 and
68 AP-3) (12). Among these, interaction with AP-2 is required to downregulate the CD4 receptor
69 from the surface of infected cells (13, 14) and target it for degradation in lysosomal
70 compartments (15, 16).

71

72 HIV-1 Vpu is a small type-I transmembrane protein of 16 kDa produced late in the viral
73 replication cycle (17, 18) and contains a short luminal N-terminal peptide followed by a single
74 helical transmembrane domain and a C-terminal cytoplasmic domain (19-21). The cytoplasmic
75 domain is comprised of two α-helices linked by a flexible loop known for its interaction with the
76 $SCF^{\beta TRCP}$ E3 ubiquitin ligase complex via a conserved phosphoserine motif ($DS^{P}GNES^{P}$) (22,
77 23). Vpu mainly localizes within intracellular compartments, notably the endoplasmic reticulum
78 (ER) and the *trans*-Golgi network (TGN) (24-26). Like Nef, Vpu also induces degradation of
79 newly synthesized CD4 by directing it through an ER-associated pathway (ERAD) for further

80 proteasomal degradation (22, 27-29). In addition, Vpu sequesters the restriction factor BST-2 in
81 the TGN using its transmembrane domain, thereby increasing the release of progeny virions (30-
82 33).
83
84 CD4 downregulation by Nef and Vpu was previously reported to be critical for efficient viral
85 replication in T cells by enhancing virion release and infectivity, and by preventing
86 superinfection (34-39). CD4 downregulation is critical for immune evasion since the anti-Env
87 antibody (Ab) response is dominated by non-neutralizing antibodies (nnAbs) that target Env in
88 its "open" CD4-bound conformation (40-42). The interaction between CD4 and Env at the
89 surface of HIV-1-infected cells has been shown to promote nnAbs binding to Env, leading to the
90 elimination of infected cells through Fc-mediated effector functions, including antibody-
91 dependant cellular cytotoxicity (ADCC) (41, 43). Nef and Vpu limit the presence of Env-CD4
92 complexes at the cell surface and thus protect infected cells against ADCC (41, 43, 44).
93
94 In previous studies, Nef and Vpu expression was mostly examined in transfected cell lines,
95 frequently using tagged proteins (30, 31, 45, 46) or by performing Western blots and
96 immunofluorescence microscopy in infected primary cells (47-52). However, both proteins are
97 small, intracellularly located and present in low amounts, rendering their detection difficult. To
98 facilitate their analysis in primary CD4+ T cells, we developed an intracellular staining technique
99 to detect Nef and Vpu expression by flow cytometry, which allows the simultaneous detection of
100 these proteins together with host and viral proteins within a single infected cell. Using this
101 method, we show that Nef and Vpu expression predicts the susceptibility of HIV-1-infected
102 primary CD4+ T cells to ADCC by HIV+ plasma. We also explain why decreased Nef

103 expression in widely-used reporter viruses increase the susceptibility of infected cells to ADCC
104 responses.
105
106 **RESULTS**
107 **Intracellular detection of Nef and Vpu in HIV-1-infected primary CD4+ T cells.**
108 To facilitate detection of intracellular Nef, we obtained a polyclonal Nef antiserum through the
109 NIH AIDS Reagent Program, which was generated by immunization of rabbits with a
110 recombinant clade B Nef consensus protein produced in *E. coli* (53). In previous studies, this
111 antibody detected native Nef proteins by Western blot and immunofluorescence microscopy in
112 both transfected and infected cells (47, 54-56). Given the scarcity of anti-Vpu antibodies, we
113 immunized rabbits with a peptide corresponding to the clade B Vpu C-terminal region (residues
114 69-81). A similar approach was previously used to generate a polyclonal antibody capable of
115 detecting Vpu by Western blot and immunofluorescence microscopy (24, 57).
116
117 We first evaluated the ability of both Nef and Vpu antisera to recognize their cognate antigen
118 using HEK 293T cells transfected with plasmids expressing the Nef or Vpu proteins from the
119 transmitted/founder (T/F) virus CH058 (58, 59). Forty-eight hours post-transfection, cells were
120 permeabilized and stained with the antisera, followed by detection with a fluorescently-labelled
121 anti-rabbit secondary antibody. As expected, the Nef antiserum recognized only Nef transfected
122 cells, while the Vpu antiserum recognized only Vpu transfected cells (Fig. 1A-C). To evaluate
123 whether our method detected Nef and Vpu when expressed in a biologically relevant culture
124 system, we infected primary CD4+ T cells with CH058 infectious molecular clones (IMC)
125 encoding Nef, and/or Vpu proteins. While wildtype (WT)-infected cells were efficiently

126 recognized by both Nef and Vpu antisera, abrogation of Nef (Fig 1D-E) or Vpu (Fig. 1F-G)
127 expression prevented the recognition of productively-infected cells as identified by Gag protein
128 intracellular staining (p24+). Of note, mock-infected or uninfected bystander cells (p24-) where
129 not detected by either antiserum, further confirming their specificity (Fig 1D-G).
130
131 We next examined the antiserum binding to Nef and Vpu proteins from different HIV-1 clades
132 and groups as well as from closely related simian immunodeficiency viruses (SIV). Primary
133 CD4+ T cells were infected with a panel of HIV-1 IMCs representing clades B, C, A1 and
134 CRF01_AE. As expected, both Nef and Vpu antisera recognized their respective antigen in cells
135 infected with clade B viruses since both were raised against clade B immunogens (Fig. 1H-I).
136 The anti-Nef polyclonal antibody was also able to recognize Nef proteins from group M clades
137 C, A1 and CRF01_AE as well as the Nef from a group O isolate. This recognition extended even
138 to the Nef protein of a related SIVcpzPts strain (isolate TAN2) but not to chimeric simian-human
139 immunodeficiency viruses (SHIV) which express a SIVmac Nef (Fig. 1H). The Vpu antiserum
140 was less cross-reactive and failed to detect Vpu from clade C viruses (Fig. 1I). These findings
141 confirmed the specificity and cross-reactivity of the intracellular detection of Nef and Vpu using
142 infected primary CD4+ T cells.
143
144 **Measuring CD4 and BST-2 downregulation in infected primary CD4+ T cells with or**
145 **without Nef and Vpu expression.**
146 The efficient detection of Nef and Vpu at the single cell level by flow cytometry allowed us to
147 combine this approach with the quantification of CD4 and BST-2 expression levels on the cell
148 surface. Productively-infected cells (p24+) expressing both Nef and Vpu had little detectable

149 CD4 and BST-2 compared to uninfected cells (Fig. 2A). In contrast, cells infected with Vpu or
150 Nef mutant viruses differed in the extent of CD4 and BST-2 downregulation (Fig. 2A).
151
152 Vpu targets CD4 and BST-2 by different mechanisms. First, Vpu interacts with multiple
153 transmembrane proteins, including BST-2, through its transmembrane domain (TMD), which
154 sequesters these proteins in perinuclear compartments (32, 33, 60-63). Second, Vpu
155 downregulates CD4 by interaction of its cytoplasmic domain with the cytoplasmic tail of CD4
156 (64-69). Consistent with these different interaction modes, Vpu-mediated CD4 and BST-2
157 degradation involves independent pathways (proteasomal and lysosomal degradation,
158 respectively), both of which depend on polyubiquitination by the $SCF^{\beta TRCP}$ E3 ubiquitin ligase
159 complex, recruited by Vpu using its highly conserved phosphoserine motif (22, 26, 70, 71). To
160 examine whether we could measure the expression and activity of Vpu mutants by flow
161 cytometry, we introduced mutations at critical residues of the Vpu TMD (A14L/A18L) or its
162 phosphoserine motif (S52A/S56A). CH058 IMCs coding for wildtype or mutated Vpu proteins
163 were used to infect primary CD4+ T cells. While the TMD mutations did not affect Vpu
164 expression, the phosphoserine mutations led to a significant accumulation of intracellular Vpu
165 proteins (Fig. 2B), most likely because Vpu is degraded together with its target protein as a
166 ubiquitinated complex (24, 72, 73). Despite a higher expression, the Vpu phosphoserine mutant
167 was unable to downregulate CD4 and marginally diminished in its capacity to antagonize BST-2
168 (Fig 2C-F). This is consistent with studies demonstrating that the recruitment of the $SCF^{\beta TRCP}$ E3
169 ubiquitin ligase complex and the degradation of BST-2 by Vpu is dissociable from its capacity to
170 antagonize the restriction factor (32, 71, 74-76). In contrast, the Vpu TMD mutations did not
171 affect Vpu's ability to target CD4 but completely abrogated its capacity to downregulate BST-2

172 (Fig 2C-F). Together, these results emphasize the need of measuring Nef and Vpu expression
173 when studying their biological functions.
174
175 **Nef and Vpu expression inversely correlates with ADCC responses.**
176 CD4 downregulation by Nef and Vpu, together with Vpu-mediated BST-2 antagonism were
177 found to be critical factors preventing the exposure of vulnerable CD4-induced Env epitopes,
178 thus protecting HIV-1-infected cells from ADCC (41, 43, 44, 77-80). To investigate the link
179 between Nef and Vpu expression and HIV-1-infected cells immune evasion, we infected
180 activated primary CD4+ T cells from five HIV-negative individuals with two clade B IMCs,
181 CH058 T/F and JR-FL, encoding functional or defective *nef* and *vpu* genes. Focusing on the
182 productively-infected cells (p24+), we performed a comprehensive characterization of the
183 patterns of viral protein expression including cell-surface Env (detected with the conformation-
184 independent Ab 2G12), intracellular Nef and Vpu in combination with cell-surface levels of CD4
185 and BST-2. We also measured the specific recognition and elimination of infected cells by
186 ADCC using the CD4-induced (CD4i) A32 monoclonal Ab (mAb). This antibody binds the
187 cluster A region of the gp120 which is occluded in the "closed" trimer and therefore can only
188 bind Env in the "open" CD4-bound conformation. We also tested 25 different plasma samples
189 from chronically HIV-1-infected individuals. As expected, Nef was only expressed by WT and
190 Vpu- constructs, while Vpu was only expressed by WT and Nef- constructs (Fig. 3A). Consistent
191 with previous reports (43, 77, 78), deletion of Nef strongly impaired CD4 downregulation by
192 both viruses but did not affect Env or BST-2 cell-surface levels. Vpu deletion mitigated CD4
193 downregulation to a lesser extent than Nef and abrogated BST-2 downmodulation, resulting in an
194 overall increase in the amount of cell-surface Env (Fig. 3B). We noticed lower levels of the JR-

195 FL Vpu protein compared to CH058 Vpu, which was linked to a less effective Vpu-mediated
196 CD4 downmodulation (Fig. 3B). The cumulative effect of Nef and Vpu on cell-surface levels of
197 Env, CD4 and BST-2 prevented the recognition of infected cells and protected them from ADCC
198 responses mediated by A32 and HIV+ plasma (Fig. 3C-D). In contrast, abrogation of Nef or Vpu
199 expression resulted in increased recognition and susceptibility of infected cells to ADCC
200 mediated by nnAbs (Fig. 3C-D). We performed correlation analyses to measure the level of
201 association between the different cellular, virological and immunological variables (Fig 3E-F).
202 We found that both Nef and Vpu established a large network of inverse correlations with cellular
203 and immunological factors. Interestingly, Env levels hardly contributed to the network and were
204 poorly associated with the immunological outcome, thus indicating that the overall amount of
205 Env present at the surface does not dictate ADCC responses mediated by CD4i Abs or HIV+
206 plasma, but rather the conformation Env occupies. Apart from antibody binding, ADCC
207 responses mediated by nnAbs correlated strongly with CD4 and Nef levels (Fig. 3E-F). Overall,
208 Nef and Vpu expression inversely correlates with the susceptibility of HIV-1-infected cells to
209 ADCC mediated by CD4i Abs and HIV+ plasma.
210

211 **Impaired Nef expression from IMC LucR.T2A constructs enhance the susceptibility of**
212 **infected cells to ADCC.**

213 Infectious molecular clones encoding for the *Renilla* luciferase (LucR) reporter gene upstream of
214 the *nef* sequence, and a T2A ribosome-skipping peptide to drive Nef expression are widely
215 employed to quantify anti-HIV-1 ADCC responses (81-92). Despite evidence that Nef-mediated
216 CD4 downregulation is impaired when using these IMCs (54, 79), a series of recent studies have
217 hypothesized that Vpu can compensate for the absence of Nef expression and completely

218 downregulate CD4 on its own (93-97). To evaluate this hypothesis, we used our intracellular
219 staining to measure Nef and Vpu expression levels and study their impact on ADCC responses
220 mediated by nnAbs against cells infected with IMC-LucR.T2A constructs. Primary CD4+ T cells
221 were infected with NL4.3-based IMCs that do (Env-IMC-LucR.T2A) or do not encode (Env-
222 IMC) a LucR.T2A cassette. These IMCs express the Env ectodomain from two clade B viruses,
223 CH058 T/F and YU-2. Consistent with the lack of Nef detection by Western blot (54, 79),
224 insertion of the LucR.T2A cassette also impaired the detection of Nef by flow cytometry, while
225 Vpu expression remained unchanged (Fig. 4A-B). However, we noted an accumulation of cell-
226 surface CD4 for Env-IMC-LucR.T2A compared to *nef*-intact constructs (~20-fold higher) (Fig.
227 4C), which resulted in a significantly increased recognition and susceptibility of infected cells to
228 ADCC responses mediated by A32 mAb and HIV+ plasma (Fig. 4D-E). Of note, both the
229 binding and the ADCC responses mediated by nnAbs were strongly associated with CD4 levels
230 and inversely correlated with Nef expression (Fig 4F-G). In contrast, these variables poorly
231 correlated with Vpu expression. Based on these data, it seems clear that Vpu expression alone is
232 not sufficient to prevent ADCC-mediated killing of infected cells and that HIV-1 requires both
233 Nef and Vpu for efficient humoral response evasion.
234

235 **Nef, Vpu and CD4 levels predict ADCC responses mediated by HIV+ plasma.**

236 We next used univariate multiple linear regression (MLR) analysis to evaluate the capacity of
237 different variables to predict ADCC responses mediated by HIV+ plasma. This model is based
238 on the hypothesis that a linear relationship exists between the dependant variable quantified
239 empirically and the independent variables that serve as predictive variables. In our model, the
240 dependant variable is the ADCC responses mediated by plasma from HIV+ donors (ADCC

241 HIV+ plasma) and the independent variables are the cellular, virological and immunological
242 factors measured on infected cells. To run the MLR model, we combined data obtained with the
243 different viral constructs (Fig. 3 & 4) and plotted the mean ADCC obtained with 25 HIV+
244 plasma against a single virus on the X axis and the associated predicted ADCC value based on
245 one or more independent variables on the Y axis. When looking at cellular factors, we noticed
246 that only CD4 accurately predicts ADCC responses mediated by HIV+ plasma, independent of
247 the viral strain (Fig. 5A). Even though BST-2 displayed a strong correlation with ADCC
248 responses (Fig 3E), it was not predictive. When focusing on virological variables, we observed
249 that Nef is the only significant ADCC predictive variable, albeit not as good as CD4 (Fig. 5A-B).
250 However, combinations of Nef with Vpu or Env increased its predictive scores, reaching similar
251 levels as CD4 when combined with Vpu (Fig. 5B). Of note, the strength of the prediction was not
252 further improved when combining all three virological variables altogether. As for
253 immunological variables, their capacity to predict ADCC by HIV+ plasma was found to be
254 equivalent or even higher than for cellular and virological factors (Fig. 5C). Indeed, the binding
255 of HIV+ plasma predicted ADCC values with a similar score as CD4 or Nef and Vpu combined,
256 while the binding of A32 predicted ADCC by HIV+ plasma even better (Fig. 5A-C). This could
257 be explained by the fact that A32-like Abs present in plasma from infected individuals are from
258 the main class of Abs (anti-cluster A Abs) mediating ADCC responses against infected cells (41,
259 80, 81, 91, 98). In line with this interpretation, ADCC mediated by A32 was found to have a
260 near-perfect predictive ability, suggesting that factors, other than antibody binding, are
261 presumably needed to fully explain the ADCC phenotypes observed (Fig. 5C).
262
263

264 **DISCUSSION**

265 Unlike simple retroviruses, HIV-1 and related SIVs encode multiple accessory proteins that
266 promote viral replication and immune evasion (99). Among them, Nef and Vpu modulate the
267 expression, trafficking, localization and function of several host cell surface proteins, including
268 the viral receptor CD4, restriction factors and homing receptors (28, 30, 31, 62, 69, 100-104).
269 They also modulate a wide range of immunoreceptors to evade immune responses mediated by
270 CD8+ T, NK and NKT cells (105-113) . Most of these host cell proteins are naturally expressed
271 on primary CD4+ T cells, the preferential target of HIV-1. The detection of Nef and Vpu has
272 previously been done in transfected cells (30, 31, 46, 48, 49, 114), which results in the
273 overexpression of the viral proteins when compared to infected primary CD4+ T cells.
274 Moreover, tagged viral proteins are frequently used to facilitate their detection (30, 31, 46, 48,
275 49, 114). Protein overexpression and/or tag insertion, have the potential to impact the trafficking
276 and functions of these accessory proteins. To study Nef and Vpu's biological activities in a
277 physiologically relevant system, we developed an intracellular staining method to detect native
278 Nef and Vpu proteins in HIV-1-infected primary CD4+ T cells by flow cytometry. Using Nef
279 and Vpu antisera, we detected both viral proteins with high specificity in cells productively
280 infected (p24+) with multiple IMCs. The Nef antiserum was cross-reactive, detecting Nef from
281 group M (clade B, C, A1 and CRF01_AE), from a group O isolate and from a closely related
282 SIVcpz strain. In contrast, the Vpu antiserum recognized only clade B Vpu proteins, consistent
283 with the fact that we used a peptide from the C-terminal region of clade B Vpu. This region is
284 highly variable among group M viruses (115). More conserved regions of Vpu map to the
285 transmembrane domain of the protein and the βTRCP binding site (116, 117). However, these
286 regions are either buried into the plasma membrane or occluded by cellular partners, and thus are

287 not readily accessible for antibody recognition. While the generation of a broad Vpu antiserum is
288 challenging, it may be possible to generate clade-specific Vpu antisera by immunization using
289 peptides corresponding to the C-terminal region specific for a given clade.
290
291 Nef and Vpu intracellular detection by flow cytometry represents an excellent tool to study their
292 biological activities in HIV-1-infected primary CD4+ T cells. This method allows for the
293 detection of cell-surface substrates or antibody recognition of surface Env and the concomitant
294 detection of Nef and Vpu expression within a single infected cell (Fig. 2A). Infected CD4+ T
295 cells represent the most relevant system to study the complex interplay between these two
296 accessory proteins and the wide range of host cell factors naturally expressed by T cells. Recent
297 findings revealed that modulation of BST-2 levels by type I IFN impacts the capacity of Vpu to
298 downregulate NTB-A, PVR, CD62L and Tim-3, thus reducing its polyfunctionality (63, 69). Nef
299 and Vpu also display overlapping functions, as they share the capacity to downregulate several
300 cell-surface proteins, including CD4, PVR, CD62L and CD28 (8, 56, 62, 110, 118). The
301 expression levels of one viral protein could therefore modulate the biological activities of the
302 other, making it essential to study their functions in a context where both viral proteins are
303 expressed simultaneously at physiological levels. Thus, our intracellular staining measuring
304 Nef/Vpu expression and functionality in HIV-1-infected cells represents a new approach to better
305 characterize their functional interplay.
306
307 Increasing evidence points towards Env conformation on the surface of infected cells as a critical
308 parameter of ADCC susceptibility to HIV+ plasma (41, 119-121). Non-neutralizing antibodies in
309 the plasma from HIV-1-infected individuals target epitopes that are only exposed when Env

310 interacts with cell-surface CD4, thus adopting the "open" CD4-bound conformation (41, 43). Nef
311 and Vpu contribute to protect HIV-1-infected cells from ADCC by limiting Env-CD4 interaction
312 via CD4 downregulation and BST-2 antagonism (41, 43, 44, 77, 78). Here we confirm and
313 extend previous observations by showing that Nef and Vpu expression predicts the susceptibility
314 of HIV-1-infected primary CD4+ T cells to ADCC responses. In agreement with recent studies
315 (44, 79), we found that CD4 accurately predicted the susceptibility of infected cells to ADCC
316 (Fig. 5). Given its enhanced capacity to downregulate CD4 compared to Env or Vpu (34, 41, 43,
317 118), Nef represents the main viral factor influencing ADCC responses mediated by CD4-
318 induced ligands (Fig. 5B). On the contrary, BST-2 and Env expression, alone or in combination,
319 were unable to accurately predict the susceptibility of infected cells to ADCC. These results are
320 consistent with previous reports suggesting that Env conformation rather than overall cell-
321 surface Env levels, drives ADCC responses mediated by HIV+ plasma (41, 43, 120, 121). This is
322 also in agreement with recent work showing that BST-2 upregulation by type I IFN enhances
323 cell-surface Env levels without increasing the susceptibility of infected cells to ADCC mediated
324 by HIV+ plasma, unless CD4-mimetics are used to "open-up" Env and stabilize the CD4-bound
325 conformation (122).
326
327 A series of recent studies using LucR.T2A IMCs have hypothesized that Vpu can compensate for
328 the absence of Nef expression by fully downregulating cell-surface CD4 (93-97). Our results
329 show that this is not the case. Consistent with its role in targeting CD4 already present at the
330 plasma membrane, the impact of Nef on CD4 downmodulation is more prominent (Fig. 2 & 3)
331 (34, 41, 43, 118). In its absence, Vpu was unable to fully downregulate CD4, thus sensitizing
332 infected cells to ADCC responses. These results highlight the importance of selecting full-length

333 unmutated IMCs with proper Nef and Vpu expression to generate biologically relevant ADCC
334 measurements. For example, a recent manuscript recently reported no differences in ADCC
335 susceptibility between cells infected with clade B, clade C or CRF01_AE IMCs (123) while
336 previous studies have shown otherwise (120, 124). In this article (123), the authors use
337 functionally Nef defective LucR.T2A IMCs, which results in incomplete CD4 downregulation
338 and therefore exposure of Env in its CD4-bound conformation at the cell surface (Fig. 4) (79).
339 Thus, it is not surprising that the usage of Nef defective viruses skew ADCC responses in favor
340 of nnAbs and mitigate the intrinsic differences that exists between Env from different clades.
341 Fortunately, several alternatives to the use of LucR.T2A IMCs are available to measure ADCC
342 against productively-infected cells (125), including the Infected Cell Elimination (ICE) assay,
343 which measures the loss of productively-infected cells (p24+) by flow cytometry and allows the
344 utilization of unmodified IMCs. Utilization of an NK cells resistant T cell line expressing a Tat-
345 driven luciferase reporter gene (CEM.NKr-CCR5-sLTR-Luc) as target cells also represents an
346 option (126). Finally, luciferase reporter IMCs (referred to as LucR.6ATRi IMCs) expressing
347 similar levels of Nef than those obtained with unmodified IMC are also available. These IMCs
348 utilize a modified encephalomyocarditis virus (EMCV) internal ribosome entry site (IRES)
349 element in lieu of T2A (54, 79). Thus, LucR.6ATRi reporter viruses represent a biologically
350 relevant alternative to LucR.T2A IMCs when measuring ADCC mediated by nnAbs and plasma
351 collected from infected or vaccinated individuals.
352

353 **ACKNOWLEDGMENTS**

354 The authors thank the CRCHUM BSL3 and Flow Cytometry Platforms for technical assistance,
355 Mario Legault from the FRQS AIDS and Infectious Diseases network for cohort coordination

356 and clinical samples. We thank the following collaborators for kindly providing some infectious
357 molecular clones: Dennis Burton (The Scripps Research Institute) for JR-FL, Malcom A. Martin
358 (NIAID) for $SHIV_{AD8-EO}$, George M. Shaw (UPenn) for SHIV.AE.40100 and Sodsai
359 Tovanabutra (US MHRP) for the HIV-1_{WR27}, HIV-1_{703357}, HIV-1_{40061}, HIV-1_{CM235} and HIV-
360 1_{851891} IMCs. We thank MédiMabs for their scientific and technical support during the
361 development of the Vpu antiserum. This study was supported by grants from the National
362 Institutes of Health to A.F., C.O. and J.C.K. (R01 AI148379), to A.F. (R01 AI129769 and R01
363 AI150322) and to BHH (R01 AI162646 and UM1 AI164570). This work was also partially
364 supported by 1UM1AI164562-01, co-funded by National Heart, Lung and Blood Institute,
365 National Institute of Diabetes and Digestive and Kidney Diseases, National Institute of
366 Neurological Disorders and Stroke, National Institute on Drug Abuse and the National Institute
367 of Allergy and Infectious Diseases, a CIHR foundation grant #352417, a CIHR Team grant
368 #422148 and a Canada Foundation for Innovation grant #41027 to A.F. A.F. is the recipient of a
369 Canada Research Chair on Retroviral Entry #RCHS0235 950-232424. F.K. is supported by the
370 Deutsche Forschungsgemeinschaft (CRC 1279 and SPP 1923). J.P. is the recipient of a CIHR
371 doctoral fellowship. The funders had no role in study design, data collection and analysis,
372 decision to publish, or preparation of the manuscript.
373

374 **AUTHOR CONTRIBUTIONS**

375 J.P. J.R. and A.F. conceived the study. J.P., J.R., and A.F. designed experimental approaches.
376 J.P., J.R., R.G. R.D. and A.F. performed, analyzed, and interpreted the experiments. H.M., F.K.,
377 B.H.H., J.C.K. and C.O. supplied novel/unique reagents. J.P., J.R., BHH, and A.F. wrote the
378 paper. All authors have read, edited, and approved the final manuscript.

379

380 **CONFLICT OF INTEREST**

381 The authors declare no competing interests.

382

383 **DATA AVAILABILITY**

384 Data and reagents are available upon request.

385

386

387 **METHODS**

388

389 **Ethics Statement**

390 Written informed consent was obtained from all study participants [the Montreal Primary HIV
391 Infection Cohort (127, 128) and the Canadian Cohort of HIV Infected Slow Progressors (129-
392 131), and research adhered to the ethical guidelines of CRCHUM and was reviewed and
393 approved by the CRCHUM institutional review board (ethics committee, approval number CE
394 16.164 - CA). Research adhered to the standards indicated by the Declaration of Helsinki. All
395 participants were adult and provided informed written consent prior to enrolment in accordance
396 with Institutional Review Board approval.

397

398 **Cell lines and isolation of primary cells**

399 HEK293T human embryonic kidney cells (obtained from ATCC) were grown as previously
400 described (132). Primary human PBMCs and CD4+ T cells were isolated, activated and cultured
401 as previously described (43). Briefly, PBMCs were obtained by leukapheresis from HIV-

402 negative individuals (4 males and 1 female) and CD4+ T lymphocytes were purified from resting
403 PBMCs by negative selection using immunomagnetic beads per the manufacturer's instructions
404 (StemCell Technologies, Vancouver, BC) and were activated with phytohemagglutinin-L (10
405 μg/mL) for 48 hours and then maintained in RPMI 1640 complete medium supplemented with
406 rIL-2 (100 U/mL).
407
408 **Plasmids and proviral constructs**
409 The vesicular stomatitis virus G (VSV-G)-encoding plasmid was previously described (133).
410 Transmitted/Founder (T/F) and chronic infectious molecular clones (IMCs) of patients CH040,
411 CH058, CH077, CH131, CH141, CH167, CH185, CH198, CH236, CH269, CH293, CH440,
412 CH470, CH505, CH534, CH850, CM235, MCST, REJO, RHGA, RHPA, STCO, SUMA, TRJO,
413 WARO, WITO, WR27, 40061, 703357 and 851891 were inferred, constructed, and biologically
414 characterized as previously described (120, 134-143). The IMCs encoding for HIV-1 reference
415 strains AD8, JR-FL, JR-CSF, NL4-3, YU-2 were described elsewhere (144-149). HIV-1 group O
416 (RBF206), SIVcpz (TAN2) and chimeric SIVmac/HIV-1 IMC constructs ($SHIV_{AD8-EO}$ and
417 SHIV.AE.40100) were generated as previously published (150-153). CH058 IMCs defective for
418 Vpu and/or Nef expression were previously described (58). To generate a *nef*-defective JR-FL
419 IMC, a frameshift mutation was introduced at the unique XhoI restriction site within the *nef*
420 gene, resulting in a premature stop codon at position 47. To generate *vpu*-defective JR-FL IMCs,
421 two stop-codons were introduced directly after the start-codon of *vpu* using the QuikChange II
422 XL site-directed mutagenesis protocol (Agilent Technologies, Santa Clara, CA). The presence of
423 the desired mutations was determined by automated DNA sequencing. Proviral constructs,
424 collectively referred as Env-IMCs, comprising an HIV-1 NL4.3-based isogenic backbone

425 engineered for the insertion of heterologous *env* strain sequences and expression in *cis* of full-
426 length Env (pNL.CH058.ecto and pNL.YU-2.ecto), were previously described (47). In the same
427 study, isogenic proviral constructs encoding *Renilla* luciferase (LucR) followed in frame by a
428 ribosome-skipping T2A peptide intended to drive Nef expression were also reported (collectively
429 referred to as Env-IMC-LucR.T2A) (47). Construction of plasmids encoding for CH058 Vpu and
430 CH058 Nef in the pCGCG-IRES-eGFP expression vector was previously described (58, 59).
431

432 **Viral production and infections**

433 To achieve a similar level of infection in primary $CD4^+$ T cells among the different IMCs tested,
434 VSV-G-pseudotyped HIV-1 viruses were produced and titrated as previously described (120).
435 Viruses were then used to infect activated primary CD4+ T cells from healthy HIV-1 negative
436 donors by spin infection at 800 × *g* for 1 h in 96-well plates at 25 °C.
437

438 **Antibodies and plasma**

439 The following Abs were used to assess cell-surface Env staining: A32, 2G12 (NIH AIDS
440 Reagent Program) and PGT135 (IAVI). Mouse anti-human CD4 (clone OKT4; Thermo Fisher
441 Scientific, Waltham, MA, USA) and mouse anti-human BST-2 (clone RS38E, PE-Cy7-
442 conjugated; Biolegend, San Diego, CA, USA) were also used as primary antibodies for cell-
443 surface staining. Goat anti-mouse and anti-human antibodies pre-coupled to Alexa Fluor 647
444 (Invitrogen, Rockford, IL, USA) were used as secondary antibodies in flow cytometry
445 experiments. Plasma from HIV-infected individuals were collected, heat-inactivated and
446 conserved at −80 °C until use. Rabbit antisera raised against a Nef consensus protein (NIH AIDS
447 Reagent Program) or against a Vpu C-terminal peptide (69) were used as primary antibodies in

448 intracellular staining. BrillantViolet 421 (BV421)-conjugated donkey anti-rabbit antibodies
449 (Biolegend) were used as secondary antibodies to detect Nef and Vpu antisera binding by flow
450 cytometry. To avoid any potential cross-reactivity with the anti-rabbit secondary antibodies used
451 for intracellular staining, mouse monoclonal antibodies were used to detect CD4 and BST-2
452 proteins.
453

454 **Flow cytometry analysis of cell-surface and intracellular staining**

455 Cell-surface staining of infected cells was performed as previously described (41). Binding of
456 cell-surface HIV-1 Env by anti-Env mAbs (5 µg/mL) or HIV+ plasma (1:1000 dilution) was
457 performed at 48h post-infection. Infected cells were then permeabilized using the
458 Cytofix/Cytoperm Fixation/ Permeabilization Kit (BD Biosciences, Mississauga, ON, Canada)
459 and stained intracellularly using PE-conjugated mouse anti-p24 mAb (clone KC57; Beckman
460 Coulter, Brea, CA, USA; 1:100 dilution) in combination with Nef or Vpu rabbit antisera (1:1000
461 dilution). The percentage of infected cells ($p24^{+}$) was determined by gating on the living cell
462 population according to a viability dye staining (Aqua Vivid; Thermo Fisher Scientific).
463 Alternatively, intracellular staining was assessed on 293T expressing Nef or Vpu proteins.
464 Briefly, $2x10^{6}$ 293T cells were transfected with 7ug of Nef or Vpu expressor with the calcium-
465 phosphate method. At 48 h post transfection, 293T cells were stained intracellularly with rabbit
466 antisera raised against Nef or Vpu (1:1000). Samples were acquired on an LSRII cytometer (BD
467 Biosciences), and data analysis was performed using FlowJo v10.5.3 (Tree Star, Ashland, OR,
468 USA).
469

470 **FACS-based ADCC assay**

471 Measurement of ADCC using the FACS-based assay was performed at 48h post-infection as
472 previously described (43, 119). Briefly, HIV-1-infected primary CD4+ T cells were stained with
473 AquaVivid viability dye and cell proliferation dye eFluor670 (Thermo Fisher Scientific) and
474 used as target cells. Autologous PBMC effectors cells, stained with cell proliferation dye
475 eFluor450 (Thermo Fisher Scientific), were added at an effector: target ratio of 10:1 in 96-well
476 V-bottom plates (Corning, Corning, NY). A 1:1000 final dilution of plasma or 5µg/mL of A32
477 mAb was added to appropriate wells and cells were incubated for 5 min at room temperature.
478 The plates were subsequently centrifuged for 1 min at 300 *x* g, and incubated at 37°C, 5% CO_2
479 for 5h before being fixed in a 2% PBS-formaldehyde solution. Samples were acquired on an
480 LSRII cytometer (BD Biosciences) and data analysis was performed using FlowJo v10.5.3 (Tree
481 Star). The percentage of ADCC was calculated with the following formula: (% of p24+ cells in
482 Targets plus Effectors) − (% of p24+ cells in Targets plus Effectors plus plasma) / (% of p24+
483 cells in Targets) by gating on infected lived target cells.
484
485 **Software Scripts and Visualization**
486 Correlograms were generated using the corrplot package in program R v.4.1.012 and RStudio
487 v.1.4.1106 (154, 155) . Correlation networks were created using the ggraph and igraph packages
488 in R in undirected mode, clustered based on the igraph layout "star". Edges are weighted
489 according to P-values (inversely). Edges are only shown if $P < 0.05$, and nodes without edges
490 were removed. Nodes are sized according to the r-values of connecting edges. Multiple linear
491 regression analyses were performed using the GraphPad Prism software (version 9.1.0). The
492 coefficient of determination (R^2) was used as a metric to measure the proportion of the variation
493 observed with the dependant variable that can be explained by the variation in the independent

494 variables. Since R^2 values usually increases when more predictive variables are added to the
495 model, we also measured the adjusted R^2 (adj. R^2) to account for this caveat.
496
497 **Statistical analysis**
498 Statistics were analyzed using GraphPad Prism version 9.1.0 (GraphPad, San Diego, CA, USA).
499 Every data set was tested for statistical normality and this information was used to apply the
500 appropriate (parametric or nonparametric) statistical test. P values <0.05 were considered
501 significant; significance values are indicated as * P<0.05, ** P<0.01, *** P<0.001, ****
502 P<0.0001.
503

504 **FIGURE LEGENDS**

505

506 **Figure 1. Intracellular detection of Nef and Vpu in infected primary CD4+ T cells.**

507 (**A-C**) 293T cells transfected with an empty vector or a plasmid expressing either CH058 Nef or
508 CH058 Vpu. 48 hours post-transfection, cells were permeabilized and stained with rabbit
509 polyclonal antisera raised against Nef and Vpu to detect their respective intracellular expression.
510 Antiserum binding was detected using donkey anti-rabbit BV421 secondary Abs. (**A**) Histograms
511 depicting representative staining and (**B-C**) Median fluorescence intensities (MFI) obtained for
512 multiple independent stainings using (**B**) anti-Nef or (**C**) anti-Vpu. (**D-G**) Primary CD4+T cells
513 mock-infected or infected with CH058 T/F WT, Nef- or Vpu-, were stained to detect the
514 intracellular expression of Nef or Vpu. (**D,F**) Dot plots (left) and histograms (right) depicting
515 representative (**D**) Nef and (**F**) Vpu staining. (**E,G**) The graphs show the MFI obtained from
516 different cell populations using cells from five different donors using (**E**) anti-Nef or (**G**) anti-
517 Vpu. Error bars indicate means ± standard errors of the means (SEM). Statistical significance
518 was tested using an unpaired t test or a Mann-Whitney U test based on statistical normality (*,
519 $P < 0.05$; **, $P < 0.01$; ***, $P < 0.001$; ns, nonsignificant). (**H-I**) Primary CD4+ T cells were
520 infected with a panel of viruses from different clades (A1, B, C, CRF01_AE), group (M, O) and
521 host (HIV-1, SIVcpz, SHIV). The radar plots indicate the level of specific recognition of infected
522 cells (MFI normalized to uninfected cells) using the (**H**) anti-Nef or (**I**) anti-Vpu antisera. The
523 limit of detection was determined using (**H**) cells infected with CH058 Nef- for Nef staining and
524 using (**I**) cells infected with CH058 Vpu- for Vpu staining.

525

526 **Figure 2. Concomitant detection of intracellular Nef and Vpu and cell-surface CD4 and**
527 **BST-2.**
528 Primary CD4+T cells infected with CH058 T/F WT, Nef-, Vpu-, Vpu A14L/A18L or Vpu
529 S52A/S56A viruses were stained for cell-surface CD4 and BST-2 prior to detection of
530 intracellular Nef or Vpu expression. (**A,C,E**) Contour plots depicting representative cell-surface
531 CD4 or BST-2 detection in combination with Nef or Vpu intracellular detection. Mock-infected
532 cells were used as a control and are shown in grey. (**B,D,F**) The graphs show MFIs obtained
533 from five independent experiments. Error bars indicate means ± standard errors of the means
534 (SEM). Statistical significance was tested using an unpaired t test or a Mann-Whitney U test
535 based on statistical normality (*, $P < 0.05$; **, $P < 0.01$; ***, $P < 0.001$; ns, nonsignificant).
536
537 **Figure 3. Nef and Vpu intracellular detection inversely correlates with the recognition of**
538 **infected cells and their susceptibility to ADCC responses mediated by HIV+ plasma.**
539 Primary CD4+T cells were mock-infected (grey), infected with CH058 T/F (red) or JR-FL (Blue)
540 viruses (WT, Nef-, Vpu-, Nef- Vpu-) and stained for (**A**) intracellular Nef or Vpu expression in
541 combination with (**B**) cell-surface staining of Env (using the anti-Env 2G12 mAb), CD4 and
542 BST-2. The ability of the anti-Env A32 mAb and 25 different HIV+ plasma to (**C**) recognize
543 infected cells and (**D**) eliminate infected cells by ADCC was also measured. (**A-D**) The graphs
544 show the MFI obtained on the infected (p24+) cell population using cells from five different
545 donors. Error bars indicate means ± standard errors of the means (SEM). Statistical significance
546 was tested using an unpaired t test or a Mann-Whitney U test based on statistical normality (*,
547 $P < 0.05$; **, $P < 0.01$; ***, $P < 0.001$; ns, nonsignificant). (**E**) Correlograms summarize pairwise
548 correlations among all immunological, virological and cellular variables obtained from infected

549 primary CD4+ T cells (shown in A-D). Squares are color-coded according to the magnitude of
550 the correlation coefficient (r) and the square dimensions are inversely proportional with the P-
551 values. Red squares represent a positive correlation between two variables and blue squares
552 represent negative correlations. Asterisks indicate all statistically significant correlations (*P <
553 0.05, **P < 0.01, ***P < 0.005). Correlation analysis was done using nonparametric Spearman
554 rank tests. (**F**) Correlation networks were generated using data shown in (**E**). Each node (circle)
555 represents a cellular (red), an immunological (green) or a virological (blue) feature measured on
556 infected cells. Nodes are connected with edges (lines) if they are significantly correlated (P <
557 0.05); nodes without edges were removed. Edges are weighted according to P-values (inversely).
558 Red edges represent a positive correlation between two variables and blue edges represent
559 negative correlations. Nodes are sized according to the r-values of connecting edges.
560

561 **Figure 4. Lack of Nef expression in primary CD4+ T cells infected with LucR.T2A IMCs**
562 **results in enhanced ADCC.**

563 Primary CD4+T cells mock-infected (grey) or infected with chimeric IMCs expressing CH058
564 Env (red) or YU-2 Env (green) and expressing or not the LucR reporter gene. (**A**) Dot plots
565 depicting representative stainings of intracellular Nef or Vpu expression. (**B-C**) Detection by
566 flow cytometry of (**B**) intracellular Nef or Vpu expression in combination with (**C**) cell-surface
567 staining of Env (using anti-Env mAbs 2G12 (CH058) or PGT135 (YU-2)), CD4 and BST-2. The
568 ability of the A32 mAb and 25 HIV+ plasma to (**D**) recognize infected cells and (**E**) eliminate
569 infected cells by ADCC was also measured. (**B-E**) The graphs show the MFI obtained on the
570 infected (p24+) cell population using cells from five different donors. Error bars indicate means
571 ± standard errors of the means (SEM). Statistical significance was tested using an unpaired t test

572 or a Mann-Whitney U test based on statistical normality (*, $P < 0.05$; **, $P < 0.01$; ***,
573 $P < 0.001$; ns, nonsignificant). (**F**) Correlograms summarize pairwise correlations among all
574 immunological, virological and cellular variables obtained from infected primary CD4+ T cells
575 (shown in **B-E**). Squares are color-coded according to the magnitude of the correlation
576 coefficient (r) and the square dimensions are inversely proportional with the P-values. Red
577 squares represent a positive correlation between two variables and blue squares represent
578 negative correlations. Asterisks indicate all statistically significant correlations (*$P < 0.05$, **$P <$
579 0.01, ***$P < 0.005$). Correlation analysis was done using nonparametric Spearman rank tests.
580 (**G**) Correlation networks were generated using data shown in (**F**). Each node (circle) represents
581 a cellular (red), an immunological (green) or a virological (blue) feature measured on infected
582 cells. Nodes are connected with edges (lines) if they are significantly correlated ($P < 0.05$); nodes
583 without edges were removed. Edges are weighted according to P-values (inversely). Red edges
584 represent a positive correlation between two variables and blue edges represent negative
585 correlations. Nodes are sized according to the r-values of connecting edges.
586

587 **Figure 5. Prediction of ADCC responses mediated by HIV+ plasma using multiple linear**
588 **regression models.**

589 (**A-C**) Multiple linear regression analysis to identify variables that can predict the ADCC
590 responses mediated by HIV+ plasma against primary CD4+ T cells infected by different viral
591 constructs (WT, Nef-, Vpu-, Nef-Vpu-, Env-IMC, Env-IMC-LucR.T2A) from different HIV-1
592 strains (CH058, JR-FL, YU-2). Each dot represents a single virus where the average of ADCC
593 obtained with 25 different HIV+ plasma (dependent variable) is plotted on the X axis and the
594 predicted ADCC value based on one or more independent parameters is plotted on the Y axis.

595 Predictors include (**A**) cellular variables, (**B**) virological variables and (**C**) immunological
596 variables. Multiple linear regression analyses were performed using the GraphPad Prism
597 software (version 9.1.0). P values below 0.05 are considered significant and are highlighted in
598 bold. The coefficient of multiple correlation (R^2) indicates the goodness of fit of the multiple
599 regression linear model. The adjusted R^2 (Adj. R^2) is used to compare the fits of models across
600 experiments with different numbers of data points and independent variables.
601
602

603 **REFERENCES**

604 1. Desrosiers RC, Lifson JD, Gibbs JS, Czajak SC, Howe AY, Arthur LO, Johnson RP.
605 1998. Identification of highly attenuated mutants of simian immunodeficiency virus. J
606 Virol 72:1431-7.
607 2. Dave VP, Hajjar F, Dieng MM, Haddad E, Cohen EA. 2013. Efficient BST2 antagonism
608 by Vpu is critical for early HIV-1 dissemination in humanized mice. Retrovirology 10:128.
609 3. Sato K, Misawa N, Fukuhara M, Iwami S, An DS, Ito M, Koyanagi Y. 2012. Vpu
610 augments the initial burst phase of HIV-1 propagation and downregulates BST2 and
611 CD4 in humanized mice. J Virol 86:5000-13.
612 4. Sato K, Misawa N, Iwami S, Satou Y, Matsuoka M, Ishizaka Y, Ito M, Aihara K, An DS,
613 Koyanagi Y. 2013. HIV-1 Vpr accelerates viral replication during acute infection by
614 exploitation of proliferating CD4+ T cells in vivo. PLoS Pathog 9:e1003812.
615 5. Crotti A, Neri F, Corti D, Ghezzi S, Heltai S, Baur A, Poli G, Santagostino E, Vicenzi E.
616 2006. Nef alleles from human immunodeficiency virus type 1-infected long-term-
617 nonprogressor hemophiliacs with or without late disease progression are defective in
618 enhancing virus replication and CD4 down-regulation. J Virol 80:10663-74.
619 6. Rucker E, Grivel JC, Munch J, Kirchhoff F, Margolis L. 2004. Vpr and Vpu are important
620 for efficient human immunodeficiency virus type 1 replication and CD4+ T-cell depletion
621 in human lymphoid tissue ex vivo. J Virol 78:12689-93.
622 7. Kirchhoff F, Greenough TC, Brettler DB, Sullivan JL, Desrosiers RC. 1995. Brief report:
623 absence of intact nef sequences in a long-term survivor with nonprogressive HIV-1
624 infection. N Engl J Med 332:228-32.
625 8. Haller C, Muller B, Fritz JV, Lamas-Murua M, Stolp B, Pujol FM, Keppler OT, Fackler
626 OT. 2014. HIV-1 Nef and Vpu are functionally redundant broad-spectrum modulators of
627 cell surface receptors, including tetraspanins. J Virol 88:14241-57.
628 9. Tokarev A, Guatelli J. 2011. Misdirection of membrane trafficking by HIV-1 Vpu and Nef:
629 Keys to viral virulence and persistence. Cell Logist 1:90-102.
630 10. Purcell DF, Martin MA. 1993. Alternative splicing of human immunodeficiency virus type
631 1 mRNA modulates viral protein expression, replication, and infectivity. J Virol 67:6365-
632 78.
633 11. Bentham M, Mazaleyrat S, Harris M. 2006. Role of myristoylation and N-terminal basic
634 residues in membrane association of the human immunodeficiency virus type 1 Nef
635 protein. J Gen Virol 87:563-571.
636 12. Craig HM, Reddy TR, Riggs NL, Dao PP, Guatelli JC. 2000. Interactions of HIV-1 nef
637 with the mu subunits of adaptor protein complexes 1, 2, and 3: role of the dileucine-
638 based sorting motif. Virology 271:9-17.
639 13. Chaudhuri R, Lindwasser OW, Smith WJ, Hurley JH, Bonifacino JS. 2007.
640 Downregulation of CD4 by human immunodeficiency virus type 1 Nef is dependent on
641 clathrin and involves direct interaction of Nef with the AP2 clathrin adaptor. J Virol
642 81:3877-90.
643 14. Ren X, Park SY, Bonifacino JS, Hurley JH. 2014. How HIV-1 Nef hijacks the AP-2
644 clathrin adaptor to downregulate CD4. Elife 3:e01754.
645 15. Aiken C, Konner J, Landau NR, Lenburg ME, Trono D. 1994. Nef induces CD4
646 endocytosis: requirement for a critical dileucine motif in the membrane-proximal CD4
647 cytoplasmic domain. Cell 76:853-64.
648 16. Rhee SS, Marsh JW. 1994. Human immunodeficiency virus type 1 Nef-induced down-
649 modulation of CD4 is due to rapid internalization and degradation of surface CD4. J Virol
650 68:5156-63.

651 17. Schwartz S, Felber BK, Pavlakis GN. 1992. Mechanism of translation of monocistronic
652 and multicistronic human immunodeficiency virus type 1 mRNAs. Mol Cell Biol 12:207-
653 19.
654 18. Krummheuer J, Johnson AT, Hauber I, Kammler S, Anderson JL, Hauber J, Purcell DF,
655 Schaal H. 2007. A minimal uORF within the HIV-1 vpu leader allows efficient translation
656 initiation at the downstream env AUG. Virology 363:261-71.
657 19. Wray V, Federau T, Henklein P, Klabunde S, Kunert O, Schomburg D, Schubert U.
658 1995. Solution structure of the hydrophilic region of HIV-1 encoded virus protein U (Vpu)
659 by CD and 1H NMR spectroscopy. Int J Pept Protein Res 45:35-43.
660 20. Maldarelli F, Chen MY, Willey RL, Strebel K. 1993. Human immunodeficiency virus type
661 1 Vpu protein is an oligomeric type I integral membrane protein. J Virol 67:5056-61.
662 21. Marassi FM, Ma C, Gratkowski H, Straus SK, Strebel K, Oblatt-Montal M, Montal M,
663 Opella SJ. 1999. Correlation of the structural and functional domains in the membrane
664 protein Vpu from HIV-1. Proc Natl Acad Sci U S A 96:14336-41.
665 22. Margottin F, Bour SP, Durand H, Selig L, Benichou S, Richard V, Thomas D, Strebel K,
666 Benarous R. 1998. A novel human WD protein, h-beta TrCp, that interacts with HIV-1
667 Vpu connects CD4 to the ER degradation pathway through an F-box motif. Mol Cell
668 1:565-74.
669 23. Coadou G, Evrard-Todeschi N, Gharbi-Benarous J, Benarous R, Girault JP. 2002. HIV-1
670 encoded virus protein U (Vpu) solution structure of the 41-62 hydrophilic region
671 containing the phosphorylated sites Ser52 and Ser56. Int J Biol Macromol 30:23-40.
672 24. Dube M, Roy BB, Guiot-Guillain P, Mercier J, Binette J, Leung G, Cohen EA. 2009.
673 Suppression of Tetherin-restricting activity upon human immunodeficiency virus type 1
674 particle release correlates with localization of Vpu in the trans-Golgi network. J Virol
675 83:4574-90.
676 25. Klimkait T, Strebel K, Hoggan MD, Martin MA, Orenstein JM. 1990. The human
677 immunodeficiency virus type 1-specific protein vpu is required for efficient virus
678 maturation and release. J Virol 64:621-9.
679 26. Schubert U, Strebel K. 1994. Differential activities of the human immunodeficiency virus
680 type 1-encoded Vpu protein are regulated by phosphorylation and occur in different
681 cellular compartments. J Virol 68:2260-71.
682 27. Schubert U, Anton LC, Bacik I, Cox JH, Bour S, Bennink JR, Orlowski M, Strebel K,
683 Yewdell JW. 1998. CD4 glycoprotein degradation induced by human immunodeficiency
684 virus type 1 Vpu protein requires the function of proteasomes and the ubiquitin-
685 conjugating pathway. J Virol 72:2280-8.
686 28. Willey RL, Maldarelli F, Martin MA, Strebel K. 1992. Human immunodeficiency virus type
687 1 Vpu protein induces rapid degradation of CD4. J Virol 66:7193-200.
688 29. Magadan JG, Perez-Victoria FJ, Sougrat R, Ye Y, Strebel K, Bonifacino JS. 2010.
689 Multilayered mechanism of CD4 downregulation by HIV-1 Vpu involving distinct ER
690 retention and ERAD targeting steps. PLoS Pathog 6:e1000869.
691 30. Neil SJ, Zang T, Bieniasz PD. 2008. Tetherin inhibits retrovirus release and is
692 antagonized by HIV-1 Vpu. Nature 451:425-30.
693 31. Van Damme N, Goff D, Katsura C, Jorgenson RL, Mitchell R, Johnson MC, Stephens
694 EB, Guatelli J. 2008. The interferon-induced protein BST-2 restricts HIV-1 release and is
695 downregulated from the cell surface by the viral Vpu protein. Cell Host Microbe 3:245-
696 52.
697 32. Dube M, Roy BB, Guiot-Guillain P, Binette J, Mercier J, Chiasson A, Cohen EA. 2010.
698 Antagonism of tetherin restriction of HIV-1 release by Vpu involves binding and
699 sequestration of the restriction factor in a perinuclear compartment. PLoS Pathog
700 6:e1000856.

701 33. Hauser H, Lopez LA, Yang SJ, Oldenburg JE, Exline CM, Guatelli JC, Cannon PM.
702 2010. HIV-1 Vpu and HIV-2 Env counteract BST-2/tetherin by sequestration in a
703 perinuclear compartment. Retrovirology 7:51.
704 34. Wildum S, Schindler M, Munch J, Kirchhoff F. 2006. Contribution of Vpu, Env, and Nef to
705 CD4 down-modulation and resistance of human immunodeficiency virus type 1-infected
706 T cells to superinfection. J Virol 80:8047-59.
707 35. Ding S, Gasser R, Gendron-Lepage G, Medjahed H, Tolbert WD, Sodroski J, Pazgier M,
708 Finzi A. 2019. CD4 Incorporation into HIV-1 Viral Particles Exposes Envelope Epitopes
709 Recognized by CD4-Induced Antibodies. J Virol 93.
710 36. Bour S, Perrin C, Strebel K. 1999. Cell surface CD4 inhibits HIV-1 particle release by
711 interfering with Vpu activity. J Biol Chem 274:33800-6.
712 37. Cortes MJ, Wong-Staal F, Lama J. 2002. Cell surface CD4 interferes with the infectivity
713 of HIV-1 particles released from T cells. J Biol Chem 277:1770-9.
714 38. Lama J, Mangasarian A, Trono D. 1999. Cell-surface expression of CD4 reduces HIV-1
715 infectivity by blocking Env incorporation in a Nef- and Vpu-inhibitable manner. Curr Biol
716 9:622-31.
717 39. Levesque K, Zhao YS, Cohen EA. 2003. Vpu exerts a positive effect on HIV-1 infectivity
718 by down-modulating CD4 receptor molecules at the surface of HIV-1-producing cells. J
719 Biol Chem 278:28346-53.
720 40. Decker JM, Bibollet-Ruche F, Wei X, Wang S, Levy DN, Wang W, Delaporte E, Peeters
721 M, Derdeyn CA, Allen S, Hunter E, Saag MS, Hoxie JA, Hahn BH, Kwong PD, Robinson
722 JE, Shaw GM. 2005. Antigenic conservation and immunogenicity of the HIV coreceptor
723 binding site. J Exp Med 201:1407-19.
724 41. Veillette M, Coutu M, Richard J, Batraville LA, Dagher O, Bernard N, Tremblay C,
725 Kaufmann DE, Roger M, Finzi A. 2015. The HIV-1 gp120 CD4-Bound Conformation Is
726 Preferentially Targeted by Antibody-Dependent Cellular Cytotoxicity-Mediating
727 Antibodies in Sera from HIV-1-Infected Individuals. J Virol 89:545-51.
728 42. Guan Y, Pazgier M, Sajadi MM, Kamin-Lewis R, Al-Darmarki S, Flinko R, Lovo E, Wu X,
729 Robinson JE, Seaman MS, Fouts TR, Gallo RC, DeVico AL, Lewis GK. 2013. Diverse
730 specificity and effector function among human antibodies to HIV-1 envelope glycoprotein
731 epitopes exposed by CD4 binding. Proc Natl Acad Sci U S A 110:E69-78.
732 43. Veillette M, Desormeaux A, Medjahed H, Gharsallah NE, Coutu M, Baalwa J, Guan Y,
733 Lewis G, Ferrari G, Hahn BH, Haynes BF, Robinson JE, Kaufmann DE, Bonsignori M,
734 Sodroski J, Finzi A. 2014. Interaction with cellular CD4 exposes HIV-1 envelope
735 epitopes targeted by antibody-dependent cell-mediated cytotoxicity. J Virol 88:2633-44.
736 44. Alsahafi N, Ding S, Richard J, Markle T, Brassard N, Walker B, Lewis GK, Kaufmann
737 DE, Brockman MA, Finzi A. 2016. Nef Proteins from HIV-1 Elite Controllers Are
738 Inefficient at Preventing Antibody-Dependent Cellular Cytotoxicity. J Virol 90:2993-3002.
739 45. Schaefer MR, Wonderlich ER, Roeth JF, Leonard JA, Collins KL. 2008. HIV-1 Nef
740 targets MHC-I and CD4 for degradation via a final common beta-COP-dependent
741 pathway in T cells. PLoS Pathog 4:e1000131.
742 46. Dikeakos JD, Atkins KM, Thomas L, Emert-Sedlak L, Byeon IJ, Jung J, Ahn J, Wortman
743 MD, Kukull B, Saito M, Koizumi H, Williamson DM, Hiyoshi M, Barklis E, Takiguchi M,
744 Suzu S, Gronenborn AM, Smithgall TE, Thomas G. 2010. Small molecule inhibition of
745 HIV-1-induced MHC-I down-regulation identifies a temporally regulated switch in Nef
746 action. Mol Biol Cell 21:3279-92.
747 47. Edmonds TG, Ding H, Yuan X, Wei Q, Smith KS, Conway JA, Wieczorek L, Brown B,
748 Polonis V, West JT, Montefiori DC, Kappes JC, Ochsenbauer C. 2010. Replication
749 competent molecular clones of HIV-1 expressing Renilla luciferase facilitate the analysis
750 of antibody inhibition in PBMC. Virology 408:1-13.

751 48. Atkins KM, Thomas L, Youker RT, Harriff MJ, Pissani F, You H, Thomas G. 2008. HIV-1
752 Nef binds PACS-2 to assemble a multikinase cascade that triggers major
753 histocompatibility complex class I (MHC-I) down-regulation: analysis using short
754 interfering RNA and knock-out mice. J Biol Chem 283:11772-84.
755 49. Lenassi M, Cagney G, Liao M, Vaupotic T, Bartholomeeusen K, Cheng Y, Krogan NJ,
756 Plemenitas A, Peterlin BM. 2010. HIV Nef is secreted in exosomes and triggers
757 apoptosis in bystander CD4+ T cells. Traffic 11:110-22.
758 50. Komoto S, Tsuji S, Ibrahim MS, Li YG, Warachit J, Taniguchi K, Ikuta K. 2003. The vpu
759 protein of human immunodeficiency virus type 1 plays a protective role against virus-
760 induced apoptosis in primary CD4(+) T lymphocytes. J Virol 77:10304-13.
761 51. Miyagi E, Andrew AJ, Kao S, Strebel K. 2009. Vpu enhances HIV-1 virus release in the
762 absence of Bst-2 cell surface down-modulation and intracellular depletion. Proc Natl
763 Acad Sci U S A 106:2868-73.
764 52. Chu H, Wang JJ, Qi M, Yoon JJ, Chen X, Wen X, Hammonds J, Ding L, Spearman P.
765 2012. Tetherin/BST-2 is essential for the formation of the intracellular virus-containing
766 compartment in HIV-infected macrophages. Cell Host Microbe 12:360-72.
767 53. Shugars DC, Smith MS, Glueck DH, Nantermet PV, Seillier-Moiseiwitsch F, Swanstrom
768 R. 1993. Analysis of human immunodeficiency virus type 1 nef gene sequences present
769 in vivo. J Virol 67:4639-50.
770 54. Alberti MO, Jones JJ, Miglietta R, Ding H, Bakshi RK, Edmonds TG, Kappes JC,
771 Ochsenbauer C. 2015. Optimized Replicating Renilla Luciferase Reporter HIV-1 Utilizing
772 Novel Internal Ribosome Entry Site Elements for Native Nef Expression and Function.
773 AIDS Res Hum Retroviruses 31:1278-96.
774 55. Jacob RA, Edgar CR, Prevost J, Trothen SM, Lurie A, Mumby MJ, Galbraith A, Kirchhoff
775 F, Haeryfar SMM, Finzi A, Dikeakos JD. 2021. The HIV-1 accessory protein Nef
776 increases surface expression of the checkpoint receptor Tim-3 in infected CD4(+) T
777 cells. J Biol Chem 297:101042.
778 56. Pawlak EN, Dirk BS, Jacob RA, Johnson AL, Dikeakos JD. 2018. The HIV-1 accessory
779 proteins Nef and Vpu downregulate total and cell surface CD28 in CD4(+) T cells.
780 Retrovirology 15:6.
781 57. Cohen EA, Terwilliger EF, Sodroski JG, Haseltine WA. 1988. Identification of a protein
782 encoded by the vpu gene of HIV-1. Nature 334:532-4.
783 58. Heigele A, Kmiec D, Regensburger K, Langer S, Peiffer L, Sturzel CM, Sauter D,
784 Peeters M, Pizzato M, Learn GH, Hahn BH, Kirchhoff F. 2016. The Potency of Nef-
785 Mediated SERINC5 Antagonism Correlates with the Prevalence of Primate Lentiviruses
786 in the Wild. Cell Host Microbe 20:381-91.
787 59. Kmiec D, Iyer SS, Sturzel CM, Sauter D, Hahn BH, Kirchhoff F. 2016. Vpu-Mediated
788 Counteraction of Tetherin Is a Major Determinant of HIV-1 Interferon Resistance. MBio
789 7.
790 60. Bolduan S, Hubel P, Reif T, Lodermeyer V, Hohne K, Fritz JV, Sauter D, Kirchhoff F,
791 Fackler OT, Schindler M, Schubert U. 2013. HIV-1 Vpu affects the anterograde transport
792 and the glycosylation pattern of NTB-A. Virology 440:190-203.
793 61. Bolduan S, Reif T, Schindler M, Schubert U. 2014. HIV-1 Vpu mediated downregulation
794 of CD155 requires alanine residues 10, 14 and 18 of the transmembrane domain.
795 Virology 464-465:375-384.
796 62. Vassena L, Giuliani E, Koppensteiner H, Bolduan S, Schindler M, Doria M. 2015. HIV-1
797 Nef and Vpu Interfere with L-Selectin (CD62L) Cell Surface Expression To Inhibit
798 Adhesion and Signaling in Infected CD4+ T Lymphocytes. J Virol 89:5687-700.
799 63. Prevost J, Pickering S, Mumby MJ, Medjahed H, Gendron-Lepage G, Delgado GG, Dirk
800 BS, Dikeakos JD, Sturzel CM, Sauter D, Kirchhoff F, Bibollet-Ruche F, Hahn BH, Dube
801 M, Kaufmann DE, Neil SJD, Finzi A, Richard J. 2019. Upregulation of BST-2 by Type I

802 Interferons Reduces the Capacity of Vpu To Protect HIV-1-Infected Cells from NK Cell
803 Responses. mBio 10.
804 64. Bour S, Schubert U, Strebel K. 1995. The human immunodeficiency virus type 1 Vpu
805 protein specifically binds to the cytoplasmic domain of CD4: implications for the
806 mechanism of degradation. J Virol 69:1510-20.
807 65. Chen MY, Maldarelli F, Karczewski MK, Willey RL, Strebel K. 1993. Human
808 immunodeficiency virus type 1 Vpu protein induces degradation of CD4 in vitro: the
809 cytoplasmic domain of CD4 contributes to Vpu sensitivity. J Virol 67:3877-84.
810 66. Lenburg ME, Landau NR. 1993. Vpu-induced degradation of CD4: requirement for
811 specific amino acid residues in the cytoplasmic domain of CD4. J Virol 67:7238-45.
812 67. Vincent MJ, Raja NU, Jabbar MA. 1993. Human immunodeficiency virus type 1 Vpu
813 protein induces degradation of chimeric envelope glycoproteins bearing the cytoplasmic
814 and anchor domains of CD4: role of the cytoplasmic domain in Vpu-induced degradation
815 in the endoplasmic reticulum. J Virol 67:5538-49.
816 68. Margottin F, Benichou S, Durand H, Richard V, Liu LX, Gomas E, Benarous R. 1996.
817 Interaction between the cytoplasmic domains of HIV-1 Vpu and CD4: role of Vpu
818 residues involved in CD4 interaction and in vitro CD4 degradation. Virology 223:381-6.
819 69. Prevost J, Edgar CR, Richard J, Trothen SM, Jacob RA, Mumby MJ, Pickering S, Dube
820 M, Kaufmann DE, Kirchhoff F, Neil SJD, Finzi A, Dikeakos JD. 2020. HIV-1 Vpu
821 Downregulates Tim-3 from the Surface of Infected CD4(+) T Cells. J Virol 94.
822 70. Binette J, Dube M, Mercier J, Halawani D, Latterich M, Cohen EA. 2007. Requirements
823 for the selective degradation of CD4 receptor molecules by the human
824 immunodeficiency virus type 1 Vpu protein in the endoplasmic reticulum. Retrovirology
825 4:75.
826 71. Mitchell RS, Katsura C, Skasko MA, Fitzpatrick K, Lau D, Ruiz A, Stephens EB,
827 Margottin-Goguet F, Benarous R, Guatelli JC. 2009. Vpu antagonizes BST-2-mediated
828 restriction of HIV-1 release via beta-TrCP and endo-lysosomal trafficking. PLoS Pathog
829 5:e1000450.
830 72. Gustin JK, Douglas JL, Bai Y, Moses AV. 2012. Ubiquitination of BST-2 protein by HIV-1
831 Vpu protein does not require lysine, serine, or threonine residues within the BST-2
832 cytoplasmic domain. J Biol Chem 287:14837-50.
833 73. Belaidouni N, Marchal C, Benarous R, Besnard-Guerin C. 2007. Involvement of the
834 betaTrCP in the ubiquitination and stability of the HIV-1 Vpu protein. Biochem Biophys
835 Res Commun 357:688-93.
836 74. Kueck T, Neil SJ. 2012. A cytoplasmic tail determinant in HIV-1 Vpu mediates targeting
837 of tetherin for endosomal degradation and counteracts interferon-induced restriction.
838 PLoS Pathog 8:e1002609.
839 75. Kueck T, Foster TL, Weinelt J, Sumner JC, Pickering S, Neil SJ. 2015. Serine
840 Phosphorylation of HIV-1 Vpu and Its Binding to Tetherin Regulates Interaction with
841 Clathrin Adaptors. PLoS Pathog 11:e1005141.
842 76. Mangeat B, Gers-Huber G, Lehmann M, Zufferey M, Luban J, Piguet V. 2009. HIV-1 Vpu
843 neutralizes the antiviral factor Tetherin/BST-2 by binding it and directing its beta-TrCP2-
844 dependent degradation. PLoS Pathog 5:e1000574.
845 77. Arias JF, Heyer LN, von Bredow B, Weisgrau KL, Moldt B, Burton DR, Rakasz EG,
846 Evans DT. 2014. Tetherin antagonism by Vpu protects HIV-infected cells from antibody-
847 dependent cell-mediated cytotoxicity. Proc Natl Acad Sci U S A 111:6425-30.
848 78. Alvarez RA, Hamlin RE, Monroe A, Moldt B, Hotta MT, Rodriguez Caprio G, Fierer DS,
849 Simon V, Chen BK. 2014. HIV-1 Vpu antagonism of tetherin inhibits antibody-dependent
850 cellular cytotoxic responses by natural killer cells. J Virol 88:6031-46.

851 79. Prevost J, Richard J, Medjahed H, Alexander A, Jones J, Kappes JC, Ochsenbauer C,
852 Finzi A. 2018. Incomplete Downregulation of CD4 Expression Affects HIV-1 Env
853 Conformation and Antibody-Dependent Cellular Cytotoxicity Responses. J Virol 92.
854 80. Ding S, Veillette M, Coutu M, Prevost J, Scharf L, Bjorkman PJ, Ferrari G, Robinson JE,
855 Sturzel C, Hahn BH, Sauter D, Kirchhoff F, Lewis GK, Pazgier M, Finzi A. 2016. A Highly
856 Conserved Residue of the HIV-1 gp120 Inner Domain Is Important for Antibody-
857 Dependent Cellular Cytotoxicity Responses Mediated by Anti-cluster A Antibodies. J
858 Virol 90:2127-34.
859 81. Ferrari G, Pollara J, Kozink D, Harms T, Drinker M, Freel S, Moody MA, Alam SM,
860 Tomaras GD, Ochsenbauer C, Kappes JC, Shaw GM, Hoxie JA, Robinson JE, Haynes
861 BF. 2011. An HIV-1 gp120 envelope human monoclonal antibody that recognizes a C1
862 conformational epitope mediates potent antibody-dependent cellular cytotoxicity (ADCC)
863 activity and defines a common ADCC epitope in human HIV-1 serum. J Virol 85:7029-
864 36.
865 82. Tomaras GD, Ferrari G, Shen X, Alam SM, Liao HX, Pollara J, Bonsignori M, Moody
866 MA, Fong Y, Chen X, Poling B, Nicholson CO, Zhang R, Lu X, Parks R, Kaewkungwal J,
867 Nitayaphan S, Pitisuttithum P, Rerks-Ngarm S, Gilbert PB, Kim JH, Michael NL,
868 Montefiori DC, Haynes BF. 2013. Vaccine-induced plasma IgA specific for the C1 region
869 of the HIV-1 envelope blocks binding and effector function of IgG. Proc Natl Acad Sci U
870 S A doi:10.1073/pnas.1301456110.
871 83. Pollara J, Bonsignori M, Moody MA, Liu P, Alam SM, Hwang KK, Gurley TC, Kozink DM,
872 Armand LC, Marshall DJ, Whitesides JF, Kaewkungwal J, Nitayaphan S, Pitisuttithum P,
873 Rerks-Ngarm S, Robb ML, O'Connell RJ, Kim JH, Michael NL, Montefiori DC, Tomaras
874 GD, Liao HX, Haynes BF, Ferrari G. 2014. HIV-1 vaccine-induced C1 and V2 Env-
875 specific antibodies synergize for increased antiviral activities. J Virol 88:7715-26.
876 84. Santra S, Tomaras GD, Warrier R, Nicely NI, Liao HX, Pollara J, Liu P, Alam SM, Zhang
877 R, Cocklin SL, Shen X, Duffy R, Xia SM, Schutte RJ, Pemble Iv CW, Dennison SM, Li H,
878 Chao A, Vidnovic K, Evans A, Klein K, Kumar A, Robinson J, Landucci G, Forthal DN,
879 Montefiori DC, Kaewkungwal J, Nitayaphan S, Pitisuttithum P, Rerks-Ngarm S, Robb
880 ML, Michael NL, Kim JH, Soderberg KA, Giorgi EE, Blair L, Korber BT, Moog C,
881 Shattock RJ, Letvin NL, Schmitz JE, Moody MA, Gao F, Ferrari G, Shaw GM, Haynes
882 BF. 2015. Human Non-neutralizing HIV-1 Envelope Monoclonal Antibodies Limit the
883 Number of Founder Viruses during SHIV Mucosal Infection in Rhesus Macaques. PLoS
884 Pathog 11:e1005042.
885 85. Huang Y, Ferrari G, Alter G, Forthal DN, Kappes JC, Lewis GK, Love JC, Borate B,
886 Harris L, Greene K, Gao H, Phan TB, Landucci G, Goods BA, Dowell KG, Cheng HD,
887 Bailey-Kellogg C, Montefiori DC, Ackerman ME. 2016. Diversity of Antiviral IgG Effector
888 Activities Observed in HIV-Infected and Vaccinated Subjects. J Immunol 197:4603-4612.
889 86. Costa MR, Pollara J, Edwards RW, Seaman MS, Gorny MK, Montefiori DC, Liao HX,
890 Ferrari G, Lu S, Wang S. 2016. Fc Receptor-Mediated Activities of Env-Specific Human
891 Monoclonal Antibodies Generated from Volunteers Receiving the DNA Prime-Protein
892 Boost HIV Vaccine DP6-001. J Virol 90:10362-10378.
893 87. Bradley T, Pollara J, Santra S, Vandergrift N, Pittala S, Bailey-Kellogg C, Shen X, Parks
894 R, Goodman D, Eaton A, Balachandran H, Mach LV, Saunders KO, Weiner JA, Scearce
895 R, Sutherland LL, Phogat S, Tartaglia J, Reed SG, Hu SL, Theis JF, Pinter A, Montefiori
896 DC, Kepler TB, Peachman KK, Rao M, Michael NL, Suscovich TJ, Alter G, Ackerman
897 ME, Moody MA, Liao HX, Tomaras G, Ferrari G, Korber BT, Haynes BF. 2017.
898 Pentavalent HIV-1 vaccine protects against simian-human immunodeficiency virus
899 challenge. Nat Commun 8:15711.
900 88. Meyerhoff RR, Scearce RM, Ogburn DF, Lockwood B, Pickeral J, Kuraoka M, Anasti K,
901 Eudailey J, Eaton A, Cooper M, Wiehe K, Montefiori DC, Tomaras G, Ferrari G, Alam

902 SM, Liao HX, Korber B, Gao F, Haynes BF. 2017. HIV-1 Consensus Envelope-Induced
903 Broadly Binding Antibodies. AIDS Res Hum Retroviruses 33:859-868.
904 89. Sung JA, Pickeral J, Liu L, Stanfield-Oakley SA, Lam CK, Garrido C, Pollara J,
905 LaBranche C, Bonsignori M, Moody MA, Yang Y, Parks R, Archin N, Allard B, Kirchherr
906 J, Kuruc JD, Gay CL, Cohen MS, Ochsenbauer C, Soderberg K, Liao HX, Montefiori D,
907 Moore P, Johnson S, Koenig S, Haynes BF, Nordstrom JL, Margolis DM, Ferrari G.
908 2015. Dual-Affinity Re-Targeting proteins direct T cell-mediated cytolysis of latently HIV-
909 infected cells. J Clin Invest doi:10.1172/JCI82314.
910 90. Tuyishime M, Garrido C, Jha S, Moeser M, Mielke D, LaBranche C, Montefiori D,
911 Haynes BF, Joseph S, Margolis DM, Ferrari G. 2020. Improved killing of HIV-infected
912 cells using three neutralizing and non-neutralizing antibodies. J Clin Invest 130:5157-
913 5170.
914 91. Bonsignori M, Pollara J, Moody MA, Alpert MD, Chen X, Hwang KK, Gilbert PB, Huang
915 Y, Gurley TC, Kozink DM, Marshall DJ, Whitesides JF, Tsao CY, Kaewkungwal J,
916 Nitayaphan S, Pitisuttithum P, Rerks-Ngarm S, Kim JH, Michael NL, Tomaras GD,
917 Montefiori DC, Lewis GK, Devico A, Evans DT, Ferrari G, Liao HX, Haynes BF. 2012.
918 Antibody-Dependent Cellular Cytotoxicity-Mediating Antibodies from an HIV-1 Vaccine
919 Efficacy Trial Target Multiple Epitopes and Preferentially Use the VH1 Gene Family. J
920 Virol 86:11521-32.
921 92. Cheng HD, Dowell KG, Bailey-Kellogg C, Goods BA, Love JC, Ferrari G, Alter G, Gach
922 J, Forthal DN, Lewis GK, Greene K, Gao H, Montefiori DC, Ackerman ME. 2021. Diverse
923 antiviral IgG effector activities are predicted by unique biophysical antibody features.
924 Retrovirology 18:35.
925 93. Pollara J, Jones DI, Huffman T, Edwards RW, Dennis M, Li SH, Jha S, Goodman D,
926 Kumar A, LaBranche CC, Montefiori DC, Fouda GG, Hope TJ, Tomaras GD, Staats HF,
927 Ferrari G, Permar SR. 2019. Bridging Vaccine-Induced HIV-1 Neutralizing and Effector
928 Antibody Responses in Rabbit and Rhesus Macaque Animal Models. J Virol 93.
929 94. Fisher L, Zinter M, Stanfield-Oakley S, Carpp LN, Edwards RW, Denny T, Moodie Z,
930 Laher F, Bekker LG, McElrath MJ, Gilbert PB, Corey L, Tomaras G, Pollara J, Ferrari G.
931 2019. Vaccine-Induced Antibodies Mediate Higher Antibody-Dependent Cellular
932 Cytotoxicity After Interleukin-15 Pretreatment of Natural Killer Effector Cells. Front
933 Immunol 10:2741.
934 95. Lewis GK, Ackerman ME, Scarlatti G, Moog C, Robert-Guroff M, Kent SJ, Overbaugh J,
935 Reeves RK, Ferrari G, Thyagarajan B. 2019. Knowns and Unknowns of Assaying
936 Antibody-Dependent Cell-Mediated Cytotoxicity Against HIV-1. Front Immunol 10:1025.
937 96. Easterhoff D, Pollara J, Luo K, Tolbert WD, Young B, Mielke D, Jha S, O'Connell RJ,
938 Vasan S, Kim J, Michael NL, Excler JL, Robb ML, Rerks-Ngarm S, Kaewkungwal J,
939 Pitisuttithum P, Nitayaphan S, Sinangil F, Tartaglia J, Phogat S, Kepler TB, Alam SM,
940 Wiehe K, Saunders KO, Montefiori DC, Tomaras GD, Moody MA, Pazgier M, Haynes
941 BF, Ferrari G. 2020. Boosting with AIDSVAX B/E Enhances Env Constant Region 1 and
942 2 Antibody-Dependent Cellular Cytotoxicity Breadth and Potency. J Virol 94.
943 97. Tolbert WD, Van V, Sherburn R, Tuyishime M, Yan F, Nguyen DN, Stanfield-Oakley S,
944 Easterhoff D, Bonsignori M, Haynes BF, Moody MA, Ray K, Ferrari G, Lewis GK,
945 Pazgier M. 2020. Recognition Patterns of the C1/C2 Epitopes Involved in Fc-Mediated
946 Response in HIV-1 Natural Infection and the RV114 Vaccine Trial. mBio 11.
947 98. Madani N, Princiotto AM, Mach L, Ding S, Prevost J, Richard J, Hora B, Sutherland L,
948 Zhao CA, Conn BP, Bradley T, Moody MA, Melillo B, Finzi A, Haynes BF, Smith AB, III,
949 Santra S, Sodroski J. 2018. A CD4-mimetic compound enhances vaccine efficacy
950 against stringent immunodeficiency virus challenge. Nat Commun 9:2363.
951 99. Strebel K. 2013. HIV accessory proteins versus host restriction factors. Curr Opin Virol
952 3:692-9.

953 100. Ramirez PW, Famiglietti M, Sowrirajan B, DePaula-Silva AB, Rodesch C, Barker E,
954 Bosque A, Planelles V. 2014. Downmodulation of CCR7 by HIV-1 Vpu results in
955 impaired migration and chemotactic signaling within CD4(+) T cells. Cell Rep 7:2019-30.
956 101. Usami Y, Wu Y, Gottlinger HG. 2015. SERINC3 and SERINC5 restrict HIV-1 infectivity
957 and are counteracted by Nef. Nature 526:218-23.
958 102. Rosa A, Chande A, Ziglio S, De Sanctis V, Bertorelli R, Goh SL, McCauley SM,
959 Nowosielska A, Antonarakis SE, Luban J, Santoni FA, Pizzato M. 2015. HIV-1 Nef
960 promotes infection by excluding SERINC5 from virion incorporation. Nature 526:212-7.
961 103. Liu Y, Fu Y, Wang Q, Li M, Zhou Z, Dabbagh D, Fu C, Zhang H, Li S, Zhang T, Gong J,
962 Kong X, Zhai W, Su J, Sun J, Zhang Y, Yu XF, Shao Z, Zhou F, Wu Y, Tan X. 2019.
963 Proteomic profiling of HIV-1 infection of human CD4(+) T cells identifies PSGL-1 as an
964 HIV restriction factor. Nat Microbiol 4:813-825.
965 104. Fu Y, He S, Waheed AA, Dabbagh D, Zhou Z, Trinite B, Wang Z, Yu J, Wang D, Li F,
966 Levy DN, Shang H, Freed EO, Wu Y. 2020. PSGL-1 restricts HIV-1 infectivity by
967 blocking virus particle attachment to target cells. Proc Natl Acad Sci U S A 117:9537-
968 9545.
969 105. Schwartz O, Marechal V, Le Gall S, Lemonnier F, Heard JM. 1996. Endocytosis of major
970 histocompatibility complex class I molecules is induced by the HIV-1 Nef protein. Nat
971 Med 2:338-42.
972 106. Collins KL, Chen BK, Kalams SA, Walker BD, Baltimore D. 1998. HIV-1 Nef protein
973 protects infected primary cells against killing by cytotoxic T lymphocytes. Nature
974 391:397-401.
975 107. Cerboni C, Neri F, Casartelli N, Zingoni A, Cosman D, Rossi P, Santoni A, Doria M.
976 2007. Human immunodeficiency virus 1 Nef protein downmodulates the ligands of the
977 activating receptor NKG2D and inhibits natural killer cell-mediated cytotoxicity. J Gen
978 Virol 88:242-50.
979 108. Fausther-Bovendo H, Sol-Foulon N, Candotti D, Agut H, Schwartz O, Debre P, Vieillard
980 V. 2009. HIV escape from natural killer cytotoxicity: nef inhibits NKp44L expression on
981 CD4+ T cells. AIDS 23:1077-87.
982 109. Shah AH, Sowrirajan B, Davis ZB, Ward JP, Campbell EM, Planelles V, Barker E. 2010.
983 Degranulation of natural killer cells following interaction with HIV-1-infected cells is
984 hindered by downmodulation of NTB-A by Vpu. Cell Host Microbe 8:397-409.
985 110. Matusali G, Potesta M, Santoni A, Cerboni C, Doria M. 2012. The human
986 immunodeficiency virus type 1 Nef and Vpu proteins downregulate the natural killer cell-
987 activating ligand PVR. J Virol 86:4496-504.
988 111. Apps R, Del Prete GQ, Chatterjee P, Lara A, Brumme ZL, Brockman MA, Neil S,
989 Pickering S, Schneider DK, Piechocka-Trocha A, Walker BD, Thomas R, Shaw GM,
990 Hahn BH, Keele BF, Lifson JD, Carrington M. 2016. HIV-1 Vpu Mediates HLA-C
991 Downregulation. Cell Host Microbe 19:686-95.
992 112. Moll M, Andersson SK, Smed-Sorensen A, Sandberg JK. 2010. Inhibition of lipid antigen
993 presentation in dendritic cells by HIV-1 Vpu interference with CD1d recycling from
994 endosomal compartments. Blood 116:1876-84.
995 113. Chen N, McCarthy C, Drakesmith H, Li D, Cerundolo V, McMichael AJ, Screaton GR, Xu
996 XN. 2006. HIV-1 down-regulates the expression of CD1d via Nef. Eur J Immunol 36:278-
997 86.
998 114. Pacyniak E, Gomez ML, Gomez LM, Mulcahy ER, Jackson M, Hout DR, Wisdom BJ,
999 Stephens EB. 2005. Identification of a region within the cytoplasmic domain of the
1000 subtype B Vpu protein of human immunodeficiency virus type 1 (HIV-1) that is
1001 responsible for retention in the golgi complex and its absence in the Vpu protein from a
1002 subtype C HIV-1. AIDS Res Hum Retroviruses 21:379-94.

1003 115. Sharma S, Jafari M, Bangar A, William K, Guatelli J, Lewinski MK. 2019. The C-Terminal
1004 End of HIV-1 Vpu Has a Clade-Specific Determinant That Antagonizes BST-2 and
1005 Facilitates Virion Release. J Virol 93.
1006 116. Pickering S, Hue S, Kim EY, Reddy S, Wolinsky SM, Neil SJ. 2014. Preservation of
1007 Tetherin and CD4 Counter-Activities in Circulating Vpu Alleles despite Extensive
1008 Sequence Variation within HIV-1 Infected Individuals. PLoS Pathog 10:e1003895.
1009 117. Iwami S, Sato K, Morita S, Inaba H, Kobayashi T, Takeuchi JS, Kimura Y, Misawa N,
1010 Ren F, Iwasa Y, Aihara K, Koyanagi Y. 2015. Pandemic HIV-1 Vpu overcomes intrinsic
1011 herd immunity mediated by tetherin. Sci Rep 5:12256.
1012 118. Chen BK, Gandhi RT, Baltimore D. 1996. CD4 down-modulation during infection of
1013 human T cells with human immunodeficiency virus type 1 involves independent activities
1014 of vpu, env, and nef. J Virol 70:6044-53.
1015 119. Richard J, Veillette M, Brassard N, Iyer SS, Roger M, Martin L, Pazgier M, Schon A,
1016 Freire E, Routy JP, Smith AB, III, Park J, Jones DM, Courter JR, Melillo BN, Kaufmann
1017 DE, Hahn BH, Permar SR, Haynes BF, Madani N, Sodroski JG, Finzi A. 2015. CD4
1018 mimetics sensitize HIV-1-infected cells to ADCC. Proc Natl Acad Sci U S A 112:E2687-
1019 94.
1020 120. Prevost J, Zoubchenok D, Richard J, Veillette M, Pacheco B, Coutu M, Brassard N,
1021 Parsons MS, Ruxrungtham K, Bunupuradah T, Tovanabutra S, Hwang KK, Moody MA,
1022 Haynes BF, Bonsignori M, Sodroski J, Kaufmann DE, Shaw GM, Chenine AL, Finzi A.
1023 2017. Influence of the Envelope gp120 Phe 43 Cavity on HIV-1 Sensitivity to Antibody-
1024 Dependent Cell-Mediated Cytotoxicity Responses. J Virol 91.
1025 121. Prevost J, Richard J, Ding S, Pacheco B, Charlebois R, Hahn BH, Kaufmann DE, Finzi
1026 A. 2018. Envelope glycoproteins sampling states 2/3 are susceptible to ADCC by sera
1027 from HIV-1-infected individuals. Virology 515:38-45.
1028 122. Richard J, Prevost J, von Bredow B, Ding S, Brassard N, Medjahed H, Coutu M, Melillo
1029 B, Bibollet-Ruche F, Hahn BH, Kaufmann DE, Smith AB, 3rd, Sodroski J, Sauter D,
1030 Kirchhoff F, Gee K, Neil SJ, Evans DT, Finzi A. 2017. BST-2 Expression Modulates
1031 Small CD4-Mimetic Sensitization of HIV-1-Infected Cells to Antibody-Dependent Cellular
1032 Cytotoxicity. J Virol 91.
1033 123. Mielke D, Stanfield-Oakley S, Borate B, Fisher LH, Faircloth K, Tuyishime M, Greene K,
1034 Gao H, Williamson C, Morris L, Ochsenbauer C, Tomaras G, Haynes BF, Montefiori D,
1035 Pollara J, deCamp AC, Ferrari G. 2021. Selection of HIV Envelope strains for
1036 standardized assessments of vaccine-elicited antibody-dependent cellular cytotoxicity
1037 (ADCC)-mediating antibodies. J Virol doi:10.1128/JVI.01643-21:JVI0164321.
1038 124. Prevost J, Tolbert WD, Medjahed H, Sherburn RT, Madani N, Zoubchenok D, Gendron-
1039 Lepage G, Gaffney AE, Grenier MC, Kirk S, Vergara N, Han C, Mann BT, Chenine AL,
1040 Ahmed A, Chaiken I, Kirchhoff F, Hahn BH, Haim H, Abrams CF, Smith AB, III, Sodroski
1041 J, Pazgier M, Finzi A. 2020. The HIV-1 Env gp120 Inner Domain Shapes the Phe43
1042 Cavity and the CD4 Binding Site. mBio 11.
1043 125. Richard J, Prevost J, Alsahafi N, Ding S, Finzi A. 2018. Impact of HIV-1 Envelope
1044 Conformation on ADCC Responses. Trends Microbiol 26:253-265.
1045 126. Alpert MD, Heyer LN, Williams DE, Harvey JD, Greenough T, Allhorn M, Evans DT.
1046 2012. A novel assay for antibody-dependent cell-mediated cytotoxicity against HIV-1- or
1047 SIV-infected cells reveals incomplete overlap with antibodies measured by neutralization
1048 and binding assays. J Virol 86:12039-52.
1049 127. Fontaine J, Chagnon-Choquet J, Valcke HS, Poudrier J, Roger M. 2011. High
1050 expression levels of B lymphocyte stimulator (BLyS) by dendritic cells correlate with HIV-
1051 related B-cell disease progression in humans. Blood 117:145-55.

1052 128. Fontaine J, Coutlee F, Tremblay C, Routy JP, Poudrier J, Roger M. 2009. HIV infection
1053 affects blood myeloid dendritic cells after successful therapy and despite nonprogressing
1054 clinical disease. J Infect Dis 199:1007-18.
1055 129. International HIVCS, Pereyra F, Jia X, McLaren PJ, Telenti A, de Bakker PI, Walker BD,
1056 Ripke S, Brumme CJ, Pulit SL, Carrington M, Kadie CM, Carlson JM, Heckerman D,
1057 Graham RR, Plenge RM, Deeks SG, Gianniny L, Crawford G, Sullivan J, Gonzalez E,
1058 Davies L, Camargo A, Moore JM, Beattie N, Gupta S, Crenshaw A, Burtt NP, Guiducci
1059 C, Gupta N, Gao X, Qi Y, Yuki Y, Piechocka-Trocha A, Cutrell E, Rosenberg R, Moss
1060 KL, Lemay P, O'Leary J, Schaefer T, Verma P, Toth I, Block B, Baker B, Rothchild A,
1061 Lian J, Proudfoot J, Alvino DM, Vine S, Addo MM, et al. 2010. The major genetic
1062 determinants of HIV-1 control affect HLA class I peptide presentation. Science
1063 330:1551-7.
1064 130. Kamya P, Boulet S, Tsoukas CM, Routy JP, Thomas R, Cote P, Boulassel MR, Baril JG,
1065 Kovacs C, Migueles SA, Connors M, Suscovich TJ, Brander C, Tremblay CL, Bernard N.
1066 2011. Receptor-ligand requirements for increased NK cell polyfunctional potential in slow
1067 progressors infected with HIV-1 coexpressing KIR3DL1*h/*y and HLA-B*57. J Virol
1068 85:5949-60.
1069 131. Peretz Y, Ndongala ML, Boulet S, Boulassel MR, Rouleau D, Cote P, Longpre D, Routy
1070 JP, Falutz J, Tremblay C, Tsoukas CM, Sekaly RP, Bernard NF. 2007. Functional T cell
1071 subsets contribute differentially to HIV peptide-specific responses within infected
1072 individuals: correlation of these functional T cell subsets with markers of disease
1073 progression. Clin Immunol 124:57-68.
1074 132. Finzi A, Xiang SH, Pacheco B, Wang L, Haight J, Kassa A, Danek B, Pancera M, Kwong
1075 PD, Sodroski J. 2010. Topological layers in the HIV-1 gp120 inner domain regulate gp41
1076 interaction and CD4-triggered conformational transitions. Mol Cell 37:656-67.
1077 133. Emi N, Friedmann T, Yee JK. 1991. Pseudotype formation of murine leukemia virus with
1078 the G protein of vesicular stomatitis virus. J Virol 65:1202-7.
1079 134. Salazar-Gonzalez JF, Salazar MG, Keele BF, Learn GH, Giorgi EE, Li H, Decker JM,
1080 Wang S, Baalwa J, Kraus MH, Parrish NF, Shaw KS, Guffey MB, Bar KJ, Davis KL,
1081 Ochsenbauer-Jambor C, Kappes JC, Saag MS, Cohen MS, Mulenga J, Derdeyn CA,
1082 Allen S, Hunter E, Markowitz M, Hraber P, Perelson AS, Bhattacharya T, Haynes BF,
1083 Korber BT, Hahn BH, Shaw GM. 2009. Genetic identity, biological phenotype, and
1084 evolutionary pathways of transmitted/founder viruses in acute and early HIV-1 infection.
1085 J Exp Med 206:1273-89.
1086 135. Ochsenbauer C, Edmonds TG, Ding H, Keele BF, Decker J, Salazar MG, Salazar-
1087 Gonzalez JF, Shattock R, Haynes BF, Shaw GM, Hahn BH, Kappes JC. 2012.
1088 Generation of Transmitted/Founder HIV-1 Infectious Molecular Clones and
1089 Characterization of Their Replication Capacity in CD4 T Lymphocytes and Monocyte-
1090 Derived Macrophages. J Virol 86:2715-28.
1091 136. Parrish NF, Wilen CB, Banks LB, Iyer SS, Pfaff JM, Salazar-Gonzalez JF, Salazar MG,
1092 Decker JM, Parrish EH, Berg A, Hopper J, Hora B, Kumar A, Mahlokozera T, Yuan S,
1093 Coleman C, Vermeulen M, Ding H, Ochsenbauer C, Tilton JC, Permar SR, Kappes JC,
1094 Betts MR, Busch MP, Gao F, Montefiori D, Haynes BF, Shaw GM, Hahn BH, Doms RW.
1095 2012. Transmitted/founder and chronic subtype C HIV-1 use CD4 and CCR5 receptors
1096 with equal efficiency and are not inhibited by blocking the integrin alpha4beta7. PLoS
1097 Pathog 8:e1002686.
1098 137. Parrish NF, Gao F, Li H, Giorgi EE, Barbian HJ, Parrish EH, Zajic L, Iyer SS, Decker JM,
1099 Kumar A, Hora B, Berg A, Cai F, Hopper J, Denny TN, Ding H, Ochsenbauer C, Kappes
1100 JC, Galimidi RP, West AP, Jr., Bjorkman PJ, Wilen CB, Doms RW, O'Brien M, Bhardwaj
1101 N, Borrow P, Haynes BF, Muldoon M, Theiler JP, Korber B, Shaw GM, Hahn BH. 2013.

1102 Phenotypic properties of transmitted founder HIV-1. Proc Natl Acad Sci U S A 110:6626-
1103 33.
1104 138. Fenton-May AE, Dibben O, Emmerich T, Ding H, Pfafferott K, Aasa-Chapman MM,
1105 Pellegrino P, Williams I, Cohen MS, Gao F, Shaw GM, Hahn BH, Ochsenbauer C,
1106 Kappes JC, Borrow P. 2013. Relative resistance of HIV-1 founder viruses to control by
1107 interferon-alpha. Retrovirology 10:146.
1108 139. Liao HX, Lynch R, Zhou T, Gao F, Alam SM, Boyd SD, Fire AZ, Roskin KM, Schramm
1109 CA, Zhang Z, Zhu J, Shapiro L, Mullikin JC, Gnanakaran S, Hraber P, Wiehe K, Kelsoe
1110 G, Yang G, Xia SM, Montefiori DC, Parks R, Lloyd KE, Scearce RM, Soderberg KA,
1111 Cohen M, Kamanga G, Louder MK, Tran LM, Chen Y, Cai F, Chen S, Moquin S, Du X,
1112 Joyce MG, Srivatsan S, Zhang B, Zheng A, Shaw GM, Hahn BH, Kepler TB, Korber BT,
1113 Kwong PD, Mascola JR, Haynes BF. 2013. Co-evolution of a broadly neutralizing HIV-1
1114 antibody and founder virus. Nature 496:469-76.
1115 140. Gao F, Bonsignori M, Liao HX, Kumar A, Xia SM, Lu X, Cai F, Hwang KK, Song H, Zhou
1116 T, Lynch RM, Alam SM, Moody MA, Ferrari G, Berrong M, Kelsoe G, Shaw GM, Hahn
1117 BH, Montefiori DC, Kamanga G, Cohen MS, Hraber P, Kwong PD, Korber BT, Mascola
1118 JR, Kepler TB, Haynes BF. 2014. Cooperation of B cell lineages in induction of HIV-1-
1119 broadly neutralizing antibodies. Cell 158:481-91.
1120 141. Salminen MO, Ehrenberg PK, Mascola JR, Dayhoff DE, Merling R, Blake B, Louder M,
1121 Hegerich S, Polonis VR, Birx DL, Robb ML, McCutchan FE, Michael NL. 2000.
1122 Construction and biological characterization of infectious molecular clones of HIV-1
1123 subtypes B and E (CRF01_AE) generated by the polymerase chain reaction. Virology
1124 278:103-10.
1125 142. Chenine AL, Merbah M, Wieczorek L, Molnar S, Mann B, Lee J, O'Sullivan AM, Bose M,
1126 Sanders-Buell E, Kijak GH, Herrera C, McLinden R, O'Connell RJ, Michael NL, Robb
1127 ML, Kim JH, Polonis VR, Tovanabutra S. 2018. Neutralization Sensitivity of a Novel HIV-
1128 1 CRF01_AE Panel of Infectious Molecular Clones. J Acquir Immune Defic Syndr
1129 78:348-355.
1130 143. Peachman KK, Karasavvas N, Chenine AL, McLinden R, Rerks-Ngarm S, Jaranit K,
1131 Nitayaphan S, Pitisuttithum P, Tovanabutra S, Zolla-Pazner S, Michael NL, Kim JH,
1132 Alving CR, Rao M. 2015. Identification of New Regions in HIV-1 gp120 Variable 2 and 3
1133 Loops that Bind to alpha4beta7 Integrin Receptor. PLoS One 10:e0143895.
1134 144. O'Brien WA, Koyanagi Y, Namazie A, Zhao JQ, Diagne A, Idler K, Zack JA, Chen IS.
1135 1990. HIV-1 tropism for mononuclear phagocytes can be determined by regions of
1136 gp120 outside the CD4-binding domain. Nature 348:69-73.
1137 145. Li Y, Kappes JC, Conway JA, Price RW, Shaw GM, Hahn BH. 1991. Molecular
1138 characterization of human immunodeficiency virus type 1 cloned directly from uncultured
1139 human brain tissue: identification of replication-competent and -defective viral genomes.
1140 J Virol 65:3973-85.
1141 146. Theodore TS, Englund G, Buckler-White A, Buckler CE, Martin MA, Peden KW. 1996.
1142 Construction and characterization of a stable full-length macrophage-tropic HIV type 1
1143 molecular clone that directs the production of high titers of progeny virions. AIDS Res
1144 Hum Retroviruses 12:191-4.
1145 147. Krapp C, Hotter D, Gawanbacht A, McLaren PJ, Kluge SF, Sturzel CM, Mack K, Reith E,
1146 Engelhart S, Ciuffi A, Hornung V, Sauter D, Telenti A, Kirchhoff F. 2016. Guanylate
1147 Binding Protein (GBP) 5 Is an Interferon-Inducible Inhibitor of HIV-1 Infectivity. Cell Host
1148 Microbe 19:504-14.
1149 148. Koyanagi Y, Miles S, Mitsuyasu RT, Merrill JE, Vinters HV, Chen IS. 1987. Dual infection
1150 of the central nervous system by AIDS viruses with distinct cellular tropisms. Science
1151 236:819-22.

149. Adachi A, Gendelman HE, Koenig S, Folks T, Willey R, Rabson A, Martin MA. 1986. Production of acquired immunodeficiency syndrome-associated retrovirus in human and nonhuman cells transfected with an infectious molecular clone. J Virol 59:284-91.
150. Mack K, Starz K, Sauter D, Langer S, Bibollet-Ruche F, Learn GH, Sturzel CM, Leoz M, Plantier JC, Geyer M, Hahn BH, Kirchhoff F. 2017. Efficient Vpu-Mediated Tetherin Antagonism by an HIV-1 Group O Strain. J Virol 91.
151. Takehisa J, Kraus MH, Decker JM, Li Y, Keele BF, Bibollet-Ruche F, Zammit KP, Weng Z, Santiago ML, Kamenya S, Wilson ML, Pusey AE, Bailes E, Sharp PM, Shaw GM, Hahn BH. 2007. Generation of infectious molecular clones of simian immunodeficiency virus from fecal consensus sequences of wild chimpanzees. J Virol 81:7463-75.
152. Shingai M, Donau OK, Schmidt SD, Gautam R, Plishka RJ, Buckler-White A, Sadjadpour R, Lee WR, LaBranche CC, Montefiori DC, Mascola JR, Nishimura Y, Martin MA. 2012. Most rhesus macaques infected with the CCR5-tropic SHIV(AD8) generate cross-reactive antibodies that neutralize multiple HIV-1 strains. Proc Natl Acad Sci U S A 109:19769-74.
153. Li H, Wang S, Lee FH, Roark RS, Murphy AI, Smith J, Zhao C, Rando J, Chohan N, Ding Y, Kim E, Lindemuth E, Bar KJ, Pandrea I, Apetrei C, Keele BF, Lifson JD, Lewis MG, Denny TN, Haynes BF, Hahn BH, Shaw GM. 2021. New SHIVs and Improved Design Strategy for Modeling HIV-1 Transmission, Immunopathogenesis, Prevention and Cure. J Virol doi:10.1128/JVI.00071-21.
154. R Core Team. 2013. R: A language and environment for statistical computing, R Foundation for Statistical Computing, Vienna, Austria. https://www.R-project.org/.
155. RStudio team. 2015. RStudio: Integrated Development for R, RStudio, Inc., Boston, MA. http://www.rstudio.com/.

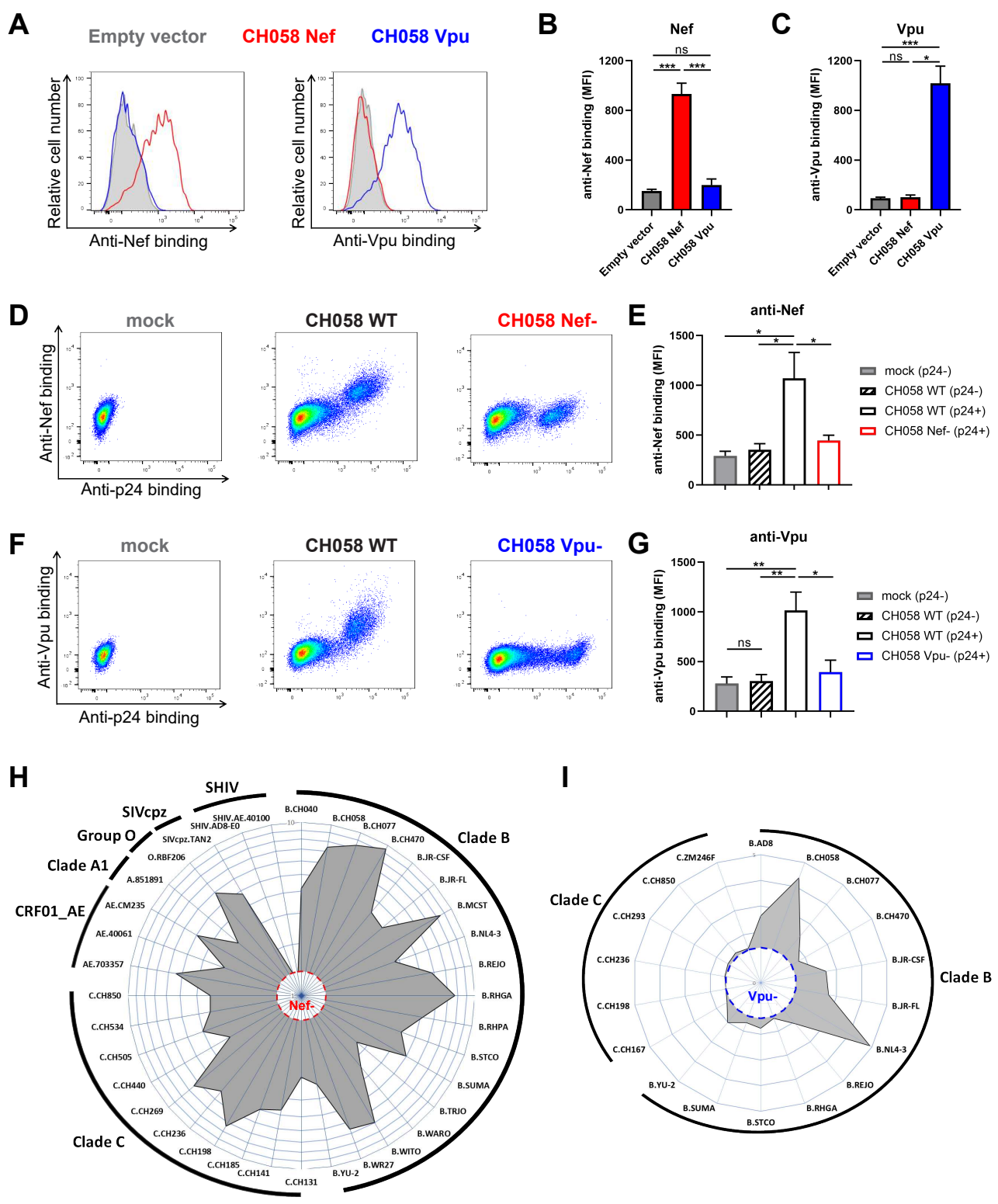
A
Empty vector
CH058 Nef
CH058 Vpu
Relative cell number
Anti-Nef binding
Anti-Vpu binding
B
Nef
anti-Nef binding (MFI)
ns
***
Empty vector
CH058 Nef
CH058 Vpu
C
Vpu
anti-Vpu binding (MFI)
***
ns
*
D
mock
CH058 WT
CH058 Nef-
Anti-Nef binding
Anti-p24 binding
E
anti-Nef
anti-Nef binding (MFI)
mock (p24-)
CH058 WT (p24-)
CH058 WT (p24+)
CH058 Nef- (p24+)
F
mock
CH058 WT
CH058 Vpu-
Anti-Vpu binding
Anti-p24 binding
G
anti-Vpu
anti-Vpu binding (MFI)
**
ns
mock (p24-)
CH058 WT (p24-)
CH058 WT (p24+)
CH058 Vpu- (p24+)
H
SHIV
SIVcpz
Group O
Clade A1
CRF01_AE
Clade B
Clade C
Nef-
I
Clade C
Clade B
Vpu-

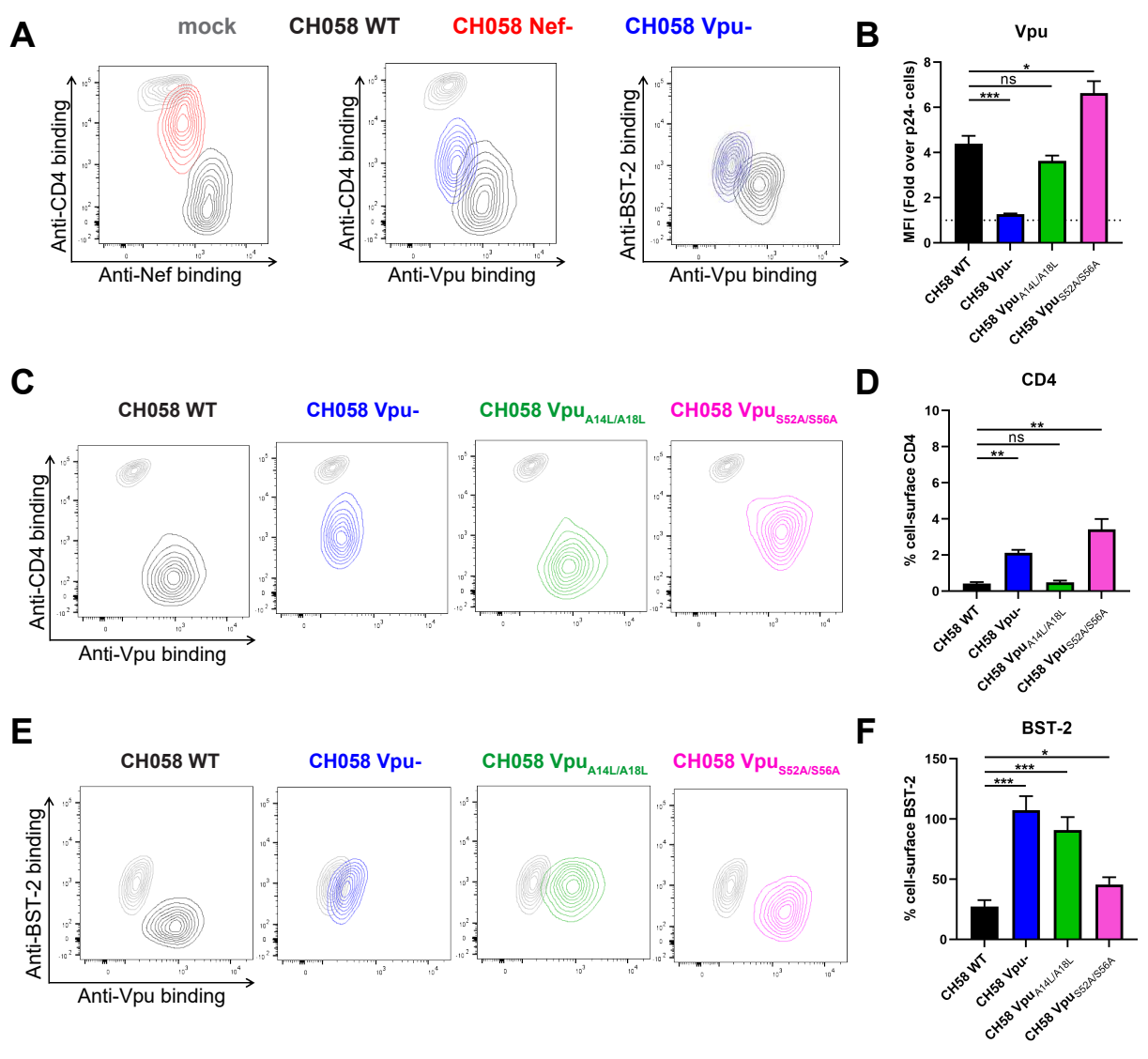
A
mock
CH058 WT
CH058 Nef-
CH058 Vpu-
Anti-CD4 binding
Anti-Nef binding
Anti-CD4 binding
Anti-Vpu binding
Anti-BST-2 binding
Anti-Vpu binding
B
Vpu
MFI (Fold over p24- cells)
*
ns
***
CH58 WT
CH58 Vpu-
CH58 VpuA14L/A18L
CH58 VpuS52A/S56A
C
CH058 WT
CH058 Vpu-
CH058 VpuA14L/A18L
CH058 VpuS52A/S56A
Anti-CD4 binding
Anti-Vpu binding
D
CD4
% cell-surface CD4
**
ns
**
CH58 WT
CH58 Vpu-
CH58 VpuA14L/A18L
CH58 VpuS52A/S56A
E
CH058 WT
CH058 Vpu-
CH058 VpuA14L/A18L
CH058 VpuS52A/S56A
Anti-BST-2 binding
Anti-Vpu binding
F
BST-2
% cell-surface BST-2
*
***
***
CH58 WT
CH58 Vpu-
CH58 VpuA14L/A18L
CH58 VpuS52A/S56A

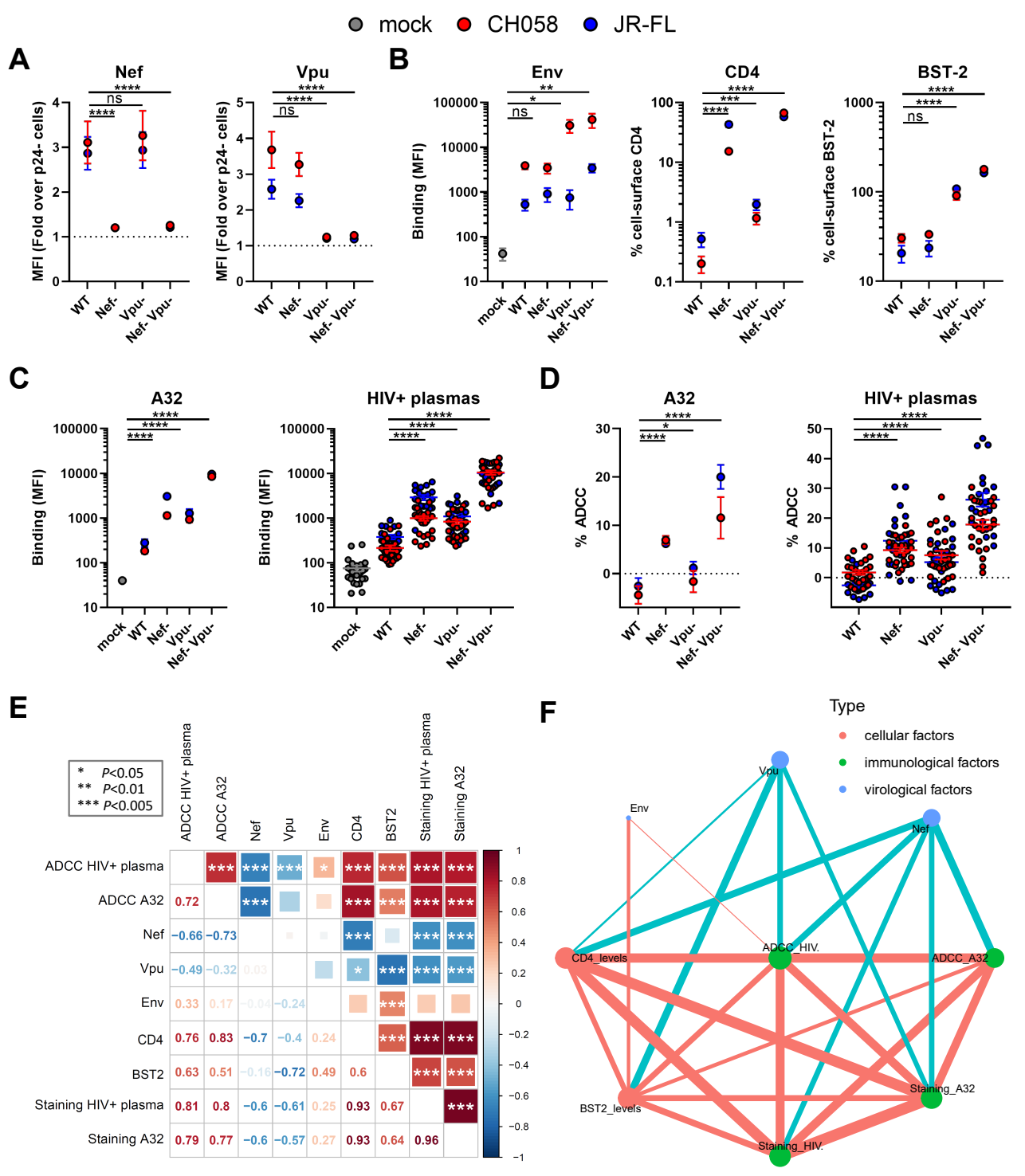
mock
CH058
JR-FL
A
Nef
Vpu
MFI (Fold over p24- cells)
WT
Nef-
Vpu-
Nef- Vpu-
B
Env
CD4
BST-2
Binding (MFI)
% cell-surface CD4
% cell-surface BST-2
C
A32
HIV+ plasmas
D
% ADCC
E
ADCC HIV+ plasma
ADCC A32
Nef
Vpu
Env
CD4
BST2
Staining HIV+ plasma
Staining A32
* P<0.05
** P<0.01
*** P<0.005
F
Type
cellular factors
immunological factors
virological factors
Vpu
Env
Nef
CD4_levels
ADCC_HIV.
ADCC_A32
Staining_A32
BST2_levels
Staining_HIV.

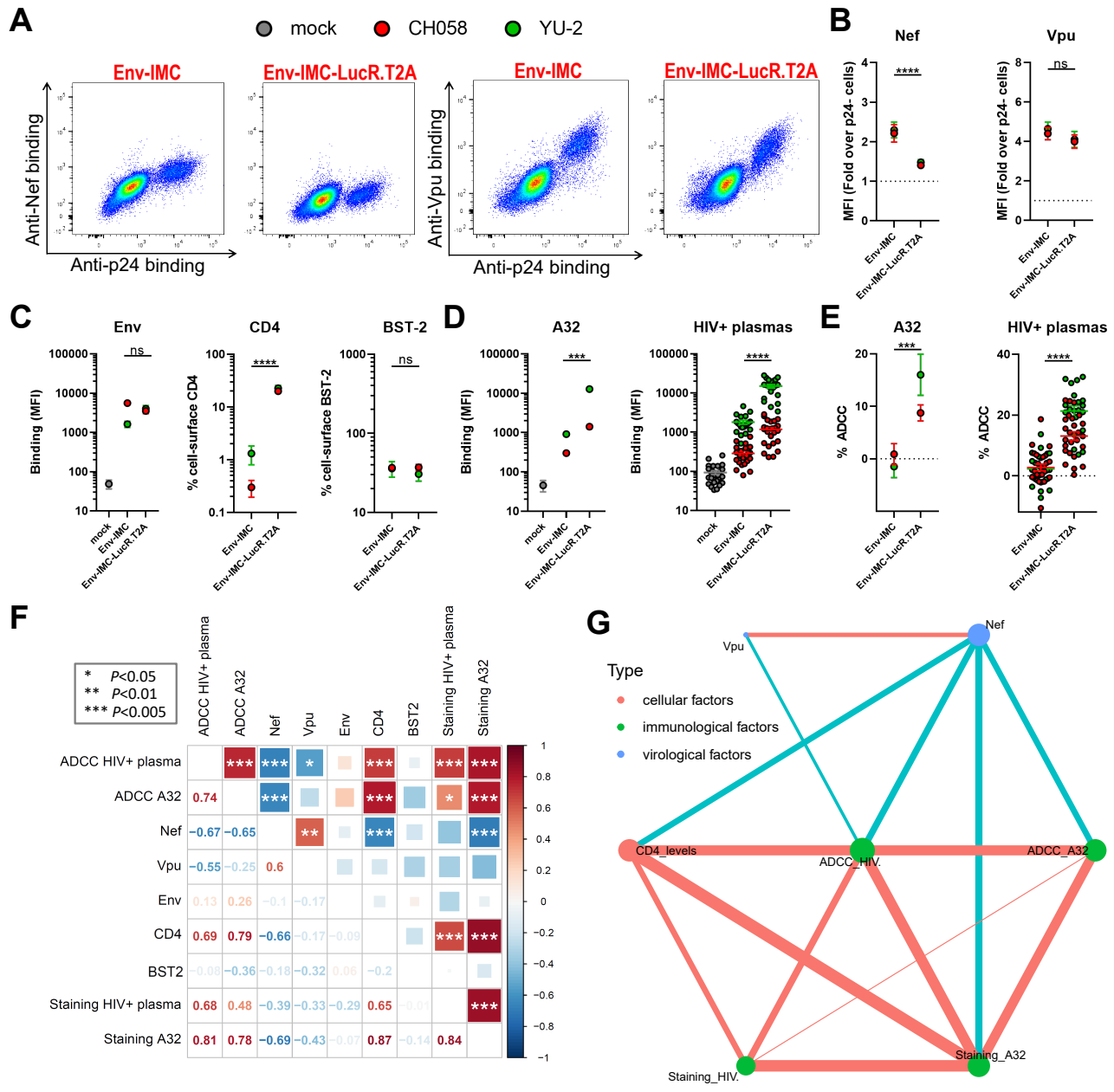
A
mock
CH058
YU-2
Env-IMC
Env-IMC-LucR.T2A
Anti-Nef binding
Anti-p24 binding
Anti-Vpu binding
B
Nef
Vpu
MFI (Fold over p24- cells)
****
ns
C
Env
CD4
BST-2
Binding (MFI)
% cell-surface CD4
% cell-surface BST-2
D
A32
HIV+ plasmas
***
E
% ADCC
F
ADCC HIV+ plasma
ADCC A32
Nef
Vpu
Env
CD4
BST2
Staining HIV+ plasma
Staining A32
* P<0.05
** P<0.01
*** P<0.005
G
Type
cellular factors
immunological factors
virological factors
CD4_levels
ADCC_HIV.
ADCC_A32
Staining_HIV.
Staining_A32

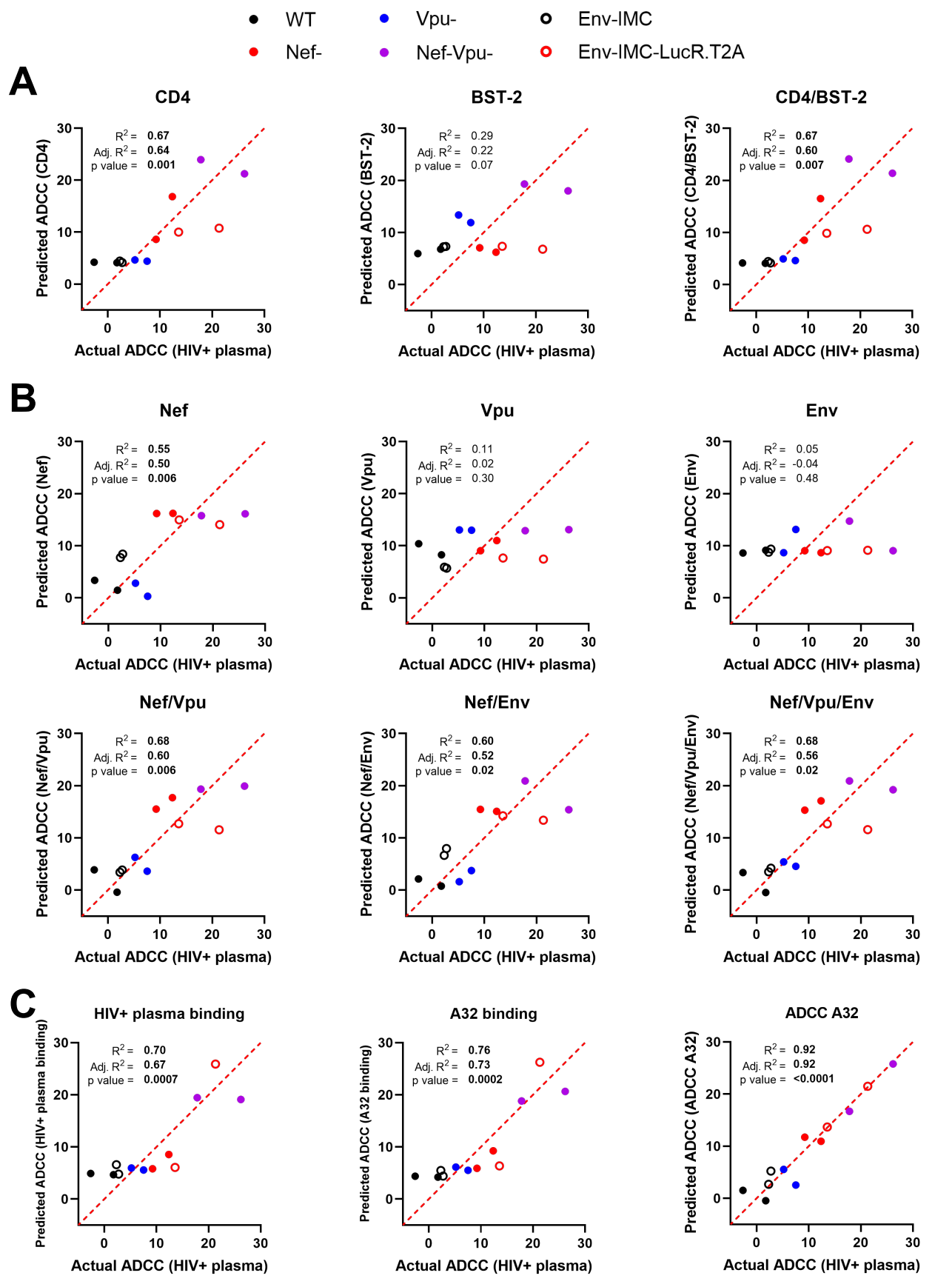
WT
Vpu-
Env-IMC
Nef-
Nef-Vpu-
Env-IMC-LucR.T2A
A
CD4
R² = 0.67
Adj. R² = 0.64
p value = 0.001
Predicted ADCC (CD4)
Actual ADCC (HIV+ plasma)
BST-2
R² = 0.29
Adj. R² = 0.22
p value = 0.07
Predicted ADCC (BST-2)
Actual ADCC (HIV+ plasma)
CD4/BST-2
R² = 0.67
Adj. R² = 0.60
p value = 0.007
Predicted ADCC (CD4/BST-2)
Actual ADCC (HIV+ plasma)
B
Nef
R² = 0.55
Adj. R² = 0.50
p value = 0.006
Predicted ADCC (Nef)
Actual ADCC (HIV+ plasma)
Vpu
R² = 0.11
Adj. R² = 0.02
p value = 0.30
Predicted ADCC (Vpu)
Actual ADCC (HIV+ plasma)
Env
R² = 0.05
Adj. R² = -0.04
p value = 0.48
Predicted ADCC (Env)
Actual ADCC (HIV+ plasma)
Nef/Vpu
R² = 0.68
Adj. R² = 0.60
p value = 0.006
Predicted ADCC (Nef/Vpu)
Actual ADCC (HIV+ plasma)
Nef/Env
R² = 0.60
Adj. R² = 0.52
p value = 0.02
Predicted ADCC (Nef/Env)
Actual ADCC (HIV+ plasma)
Nef/Vpu/Env
R² = 0.68
Adj. R² = 0.56
p value = 0.02
Predicted ADCC (Nef/Vpu/Env)
Actual ADCC (HIV+ plasma)
C
HIV+ plasma binding
R² = 0.70
Adj. R² = 0.67
p value = 0.0007
Predicted ADCC (HIV+ plasma binding)
Actual ADCC (HIV+ plasma)
A32 binding
R² = 0.76
Adj. R² = 0.73
p value = 0.0002
Predicted ADCC (A32 binding)
Actual ADCC (HIV+ plasma)
ADCC A32
R² = 0.92
Adj. R² = 0.92
p value = <0.0001
Predicted ADCC (ADCC A32)
Actual ADCC (HIV+ plasma)